Geosphere-Biosphere Interactions in *Bio-Activity* Volcanic Lakes: Evidences from Hule and Rìo Cuarto (Costa Rica)

Jacopo Cabassi[1]*, Franco Tassi[1,2], Francesca Mapelli[3], Sara Borin[3], Sergio Calabrese[4], Dmitri Rouwet[5], Giovanni Chiodini[6], Ramona Marasco[3], Bessem Chouaia[3], Rosario Avino[6], Orlando Vaselli[1,2], Giovannella Pecoraino[7], Francesco Capecchiacci[1,2], Gabriele Bicocchi[1], Stefano Caliro[6], Carlos Ramirez[8], Raul Mora-Amador[8]

1 Dipartimento di Scienze della Terra, University of Florence, Florence, Italy, 2 CNR – Istituto di Geoscienze e Georisorse, Florence, Italy, 3 Department of Food, Environmental and Nutritional Sciences, University of Milan, Milan, Italy, 4 Dipartimento di Scienze della Terra e del Mare, University of Palermo, Palermo, Italy, 5 Istituto Nazionale di Geofisica e Vulcanologia, Sezione di Bologna, Bologna, Italy, 6 Istituto Nazionale di Geofisica e Vulcanologia, Osservatorio Vesuviano, Naples, Italy, 7 Istituto Nazionale di Geofisica e Vulcanologia, Sezione di Palermo, Palermo, Italy, 8 Centro de Investigaciones en Ciencias Geológicas, Escuela Centroamericana de Geología, Red Sismológica Nacional, Universidad de Costa Rica, San Jose, Costa Rica

Abstract

Hule and Río Cuarto are maar lakes located 11 and 18 km N of Poás volcano along a 27 km long fracture zone, in the Central Volcanic Range of Costa Rica. Both lakes are characterized by a stable thermic and chemical stratification and recently they were affected by fish killing events likely related to the uprising of deep anoxic waters to the surface caused by rollover phenomena. The vertical profiles of temperature, pH, redox potential, chemical and isotopic compositions of water and dissolved gases, as well as prokaryotic diversity estimated by DNA fingerprinting and massive 16S rRNA pyrosequencing along the water column of the two lakes, have highlighted that different bio-geochemical processes occur in these meromictic lakes. Although the two lakes host different bacterial and archaeal phylogenetic groups, water and gas chemistry in both lakes is controlled by the same prokaryotic functions, especially regarding the CO_2-CH_4 cycle. Addition of hydrothermal CO_2 through the bottom of the lakes plays a fundamental priming role in developing a stable water stratification and fuelling anoxic bacterial and archaeal populations. Methanogens and methane oxidizers as well as autotrophic and heterotrophic aerobic bacteria responsible of organic carbon recycling resulted to be stratified with depth and strictly related to the chemical-physical conditions and availability of free oxygen, affecting both the CO_2 and CH_4 chemical concentrations and their isotopic compositions along the water column. Hule and Río Cuarto lakes were demonstrated to contain a CO_2 (CH_4, N_2)-rich gas reservoir mainly controlled by the interactions occurring between geosphere and biosphere. Thus, we introduced the term of *bio-activity* volcanic lakes to distinguish these lakes, which have analogues worldwide (e.g. Kivu: D.R.C.-Rwanda; Albano, Monticchio and Averno: Italy; Pavin: France) from volcanic lakes only characterized by geogenic CO_2 reservoir such as Nyos and Monoun (Cameroon).

Introduction

Volcanic lakes are peculiar natural systems on Earth, although they are a common feature of volcanic systems characterized by recent activity, being present in 476 volcanic structures worldwide (VHub, CVL Group page; [1]). A volcanic lake simultaneously acts as both a calorimeter and a condenser for acidic volatiles from magmatic and hydrothermal degassing [2–6]. Thus, its existence and durability strictly depends on the balance between i) inputs of meteoric water and hydrothermal-magmatic fluids and ii) losses related to evaporation, permeation through sediments and streaming [7]. Volcanic lakes were basically classified, as follows [1,4]: i) "high-activity" lakes affected by the addition of significant amounts of hot and hyperacidic hydrothermal–magmatic fluids; ii) "low-activity" lakes, characterized by CO_2-dominated fluid inputs at a relatively low rate from sub-lacustrine fluids discharges, favoring the establishment of a stable vertical stratification and possibly the accumulation of high amounts of dissolved gases in the deep water layers. At these conditions, a lake overturn triggered by either i) external events, such as earthquakes, landslides or extreme

weather conditions or ii) the progressive attainment of gas saturation conditions may cause the abrupt release of toxic gas clouds in the atmosphere. This phenomenon, also known as "limnic eruption", was firstly documented at Monoun and Nyos lakes (Cameroon) in 1984 and 1986, respectively [8–15]. Accordingly, low activity lakes are commonly indicated as "Nyos-type" lakes.

In Costa Rica, volcanic lakes are found in quiescent systems (Congo and Barva), as well as in volcanoes characterized by moderate hydrothermal activity (Irazú and Tenorio) and strong magmatic fluid emissions (Rincón de la Vieja and Poás) [16,17]. Hule and Río Cuarto are low-activity, Nyos-type, maar lakes located at 11 and 18 km N of Poás volcano (Fig. 1), respectively, in relation of a 27 km long fracture zone passing through the Sabana Redonda cinder cones, the Poás summit craters (Botos, Active Crater and Von Frantzius) and the Congo stratocone [18]. In these two lakes, changes in the water color and fish death events were repeatedly reported, suggesting the occurrence of rollover episodes related to inputs of deep-originated gases [18]. To the best of our knowledge, no information is available on these lakes for chemical and isotopic compositions of dissolved gases deriving from geogenic sources and the structure of prokaryotic communities. The latter are expected to play pivotal ecological functions, encompassing nutrient remineralization and carbon cycling, which is firmly linked to the fate of dissolved C_1 gases, i.e. CH_4 and CO_2.

This paper presents the geochemical (water and dissolved gas chemistry) and microbiological results obtained from samples collected in 2010 during the 7th Workshop of the Commission on Volcanic Lakes (CVL; Costa Rica 10–21 March 2010), which is part of the International Association of Volcanology and Chemistry of the Earth's Interior (IAVCEI), by a group of geochemists, limnologists, biologists and volcanologists from different universities and scientific institutions. The aim of this multidisciplinary research was to unravel the bio-geochemical processes controlling the physical-chemical features of Hule and Río Cuarto lakes along the vertical profiles, showing their implications for lake stratification and stability, and proposing evidences for a new classification system.

Morphological and Limnological Outlines

2.1 Morphological features

Lake Hule ($10°17'42''$N, $84°12'37''$W) lies within the $2.3×1.8$ km wide Hule basin, a volcanic depression also hosting Lake Congo to the north, which is separated from Lake Hule by a volcanic cone, and Lake Bosque Alegre (unofficial name) [18–20]. Lake Hule has a half-moon shape, a surface area of about $5.5×10^5$ m^2, an estimated water volume of $6.9×10^6$ m^3, and a maximum depth of ~23 m [17,18,21,22] (Fig. 2). The northern shoreline of the lake shows three tributaries, whereas an emissary (Río Hule) is located to the NE [18,23,24].

Río Cuarto maar ($10°21'23''$N, $84°13'00''$W) has a rim whose maximum elevation is ~52 m a.s.l. Lake Río Cuarto shows steep sided walls and a flat bottom, a morphology typical of maar lakes. The lake has an E-W axis of 758 m, a mean width of 581 m, a surface of $3.3×10^5$ m^2 and a water volume of $15×10^6$ m^3 [18,25] (Fig. 3). Río Cuarto is the deepest (~67 m) natural lake in Costa Rica [19]. A small tributary is located on the eastern shore, whereas no emissaries were recognized [25].

The main morphological features of Hule and Río Cuarto lakes can be summarized using the "depth-ratio" [26], which is a dimensionless parameter equal to the ratio between the average depth (the volume divided by the surface area of the lake) and the maximum depth of the lake. The obtained results are 0.55 and

0.68, respectively, for Lake Hule and Lake Río Cuarto, corresponding to an average depth of 12.6 and 45.5 m. According to Carpenter's heuristic classification [26], the depth-ratio values are consistent with the so-called ellipsoid shape (typical values comprised between 0.5 and 0.66), considered a common feature for volcanic lake basins, even though Río Cuarto morphometry tends to approximate a steep-sided frustum model, corresponding to steep sides and flat bottom [27]. Such morphological features tend to prevent water vertical mixing, favoring meromictic conditions [28]. Thus, these physical parameters have a strong influence on the vertical distribution of chemical species, especially approaching the lake bottom where bio-geochemical processes have their maximum efficiency [29].

2.2 Limnological features and rollover events

At Lake Hule, the limit between epi- and hypolimnion, marked by a very weak thermocline and the complete depletion of O_2, was reported to occur at a depth ranging between -10 and -12 m [23,24]. As reported by [22], this lake shows a persistent vertical stratification and the presence of CO_2 in the deepest water strata. Occurrence of fish death episodes, associated with sudden changes of water color from dark blue to red and strong smell in the lake surroundings, were reported by the local population in the last years (4 to 5 events from 1989 to 2002). These events, which took place during the cool, rainy and windy season (i.e. from December to February), were interpreted as caused by rollover phenomena [16,17,18,30].

The transition between epilimnion and hypolimnion in the meromictic Lake Río Cuarto was measured at 20 and 25 m depth in May-June and January-February, respectively [18,25]. Rollover events, testified by fish killing and color changes of lake water from green to yellow-reddish, were observed in 1920 [31], between 1978 and 1991 [22], in January 1997 [16] and in February 2010 [18], just one month before our sampling. These events were possibly triggered by cooling of the shallow water layer caused by an anomalous weather characterized by low air temperature and strong winds [18,25,32].

Materials and Methods

3.1 Sampling of water and dissolved gases

Water and dissolved gas sampling was carried out in March 2010 along vertical profiles from the lake surface to the bottom at regular intervals of 5 m (Lake Hule) and 10 m (Lake Río Cuarto), in sites corresponding to the deepest points. Permission to sample in both lakes was guaranteed by Red Sismológica Nacional and Universidad de Costa Rica. According to the *single hose* method [33–35], water and dissolved gas samples were collected using a sampling line consisting of 10 m long Rilsan tubes ($\Phi = 6$ mm) connected among them by steel connectors. Once the tube end was lowered to the chosen depth, water was pumped up to the surface through the sampling line using a 150 mL glass syringe equipped with a three-way teflon valve and transferred into plastic bottles after the displacement of a water volume double than the inner volume of the tube. One filtered (0.45 μm) and two filtered-acidified (with ultrapure HCl and HNO_3, respectively) water samples were collected in polyethylene bottles for the analysis of anions, cations and trace species, respectively. A fourth water aliquot was collected in glass bottles with the addition of $HgCl_2$ for the analysis of water isotopes and $^{13}C/^{12}C$ ratios of total dissolved inorganic carbon (TDIC). Five hundred mL of water were filtered immediately after the sampling recovery through sterile cellulose mixed esters 0.22 μm pore size filters (GSWP, Millipore, USA) for the analysis of prokaryotic populations. The filters were stored at
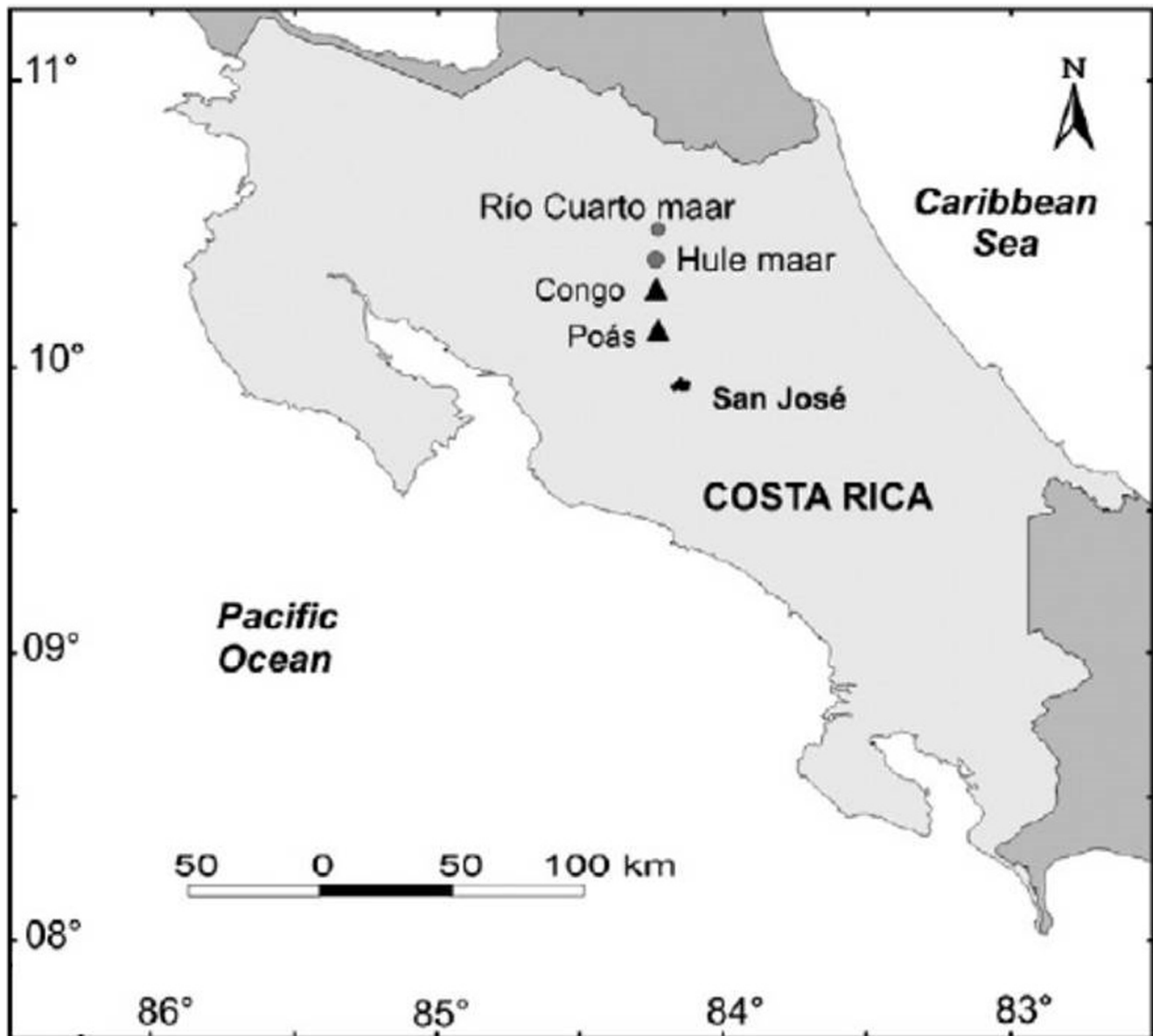
Figure 1. Map of Costa Rica with the location of Hule and Río Cuarto lakes. Modified after Alvarado *et al.* [18].
doi:10.1371/journal.pone.0102456.g001

−20°C in RNAlater solution (Quiagen, Italy), to prevent nucleic acid degradation. Dissolved gases were sampled using pre-evacuated 250 mL glass vials equipped with a Teflon stopcock and connected to the sampling line used to collect water samples. Sampling flasks were filled with water up to ¾ of the inner volume [36–38].

3.2 Field measurements

Water depth (m), temperature (°C), pH, Eh and electrical conductivity (EC; $\mu S\ cm^{-1}$) along the lake vertical profiles were measured using a Hydrolab MiniSonde 5 equipped with a data logger for data storage. The nominal precisions were: depth ±0.05 m; T±0.1°C; pH±0.2; Eh±20 mV; EC±1 $\mu S\ cm^{-1}$. Alkalinity was measured *in situ* by acidimetric titration using 0.01 N HCl. The analytical error for alkalinity analysis was ≤5%.

3.3 Chemical and isotopic analysis of water and dissolved gases

Main anions (Cl^-, SO_4^{2-}, NO_3^-, Br^- and F^-) and cations (Na^+, K^+, Ca^{2+}, Mg^{2+}, NH_4^+ and Li^+) were analyzed by ion-chromatography (IC) using Metrohm 761 and Metrohm 861 chromatographs, respectively. The analytical error for major water constituents was ≤5%. Trace elements at selected depths were analyzed at the INGV of Palermo by Inductively Coupled Plasma Mass spectrometry (ICP-MS, Agilent 7500-ce). For most of the elements the analytical uncertainty was in the order of 5-10% [39].

The $^{18}O/^{16}O$ and $^2H/^1H$ isotopic ratios of water (expressed as $\delta^{18}O$-H_2O and δD-H_2O ‰ vs. V-SMOW, respectively) from selected depths were analyzed using a Finnigan Delta plusXP continuous-flow mass spectrometer (MS) coupled with a Gas-benchII gas-chromatographic device (GBII), according to equilibration techniques with CO_2 for oxygen [40], and with H_2 for

Figure 2. Panoramic view and bathymetric map of Lake Hule (modified after Göcke [24]).
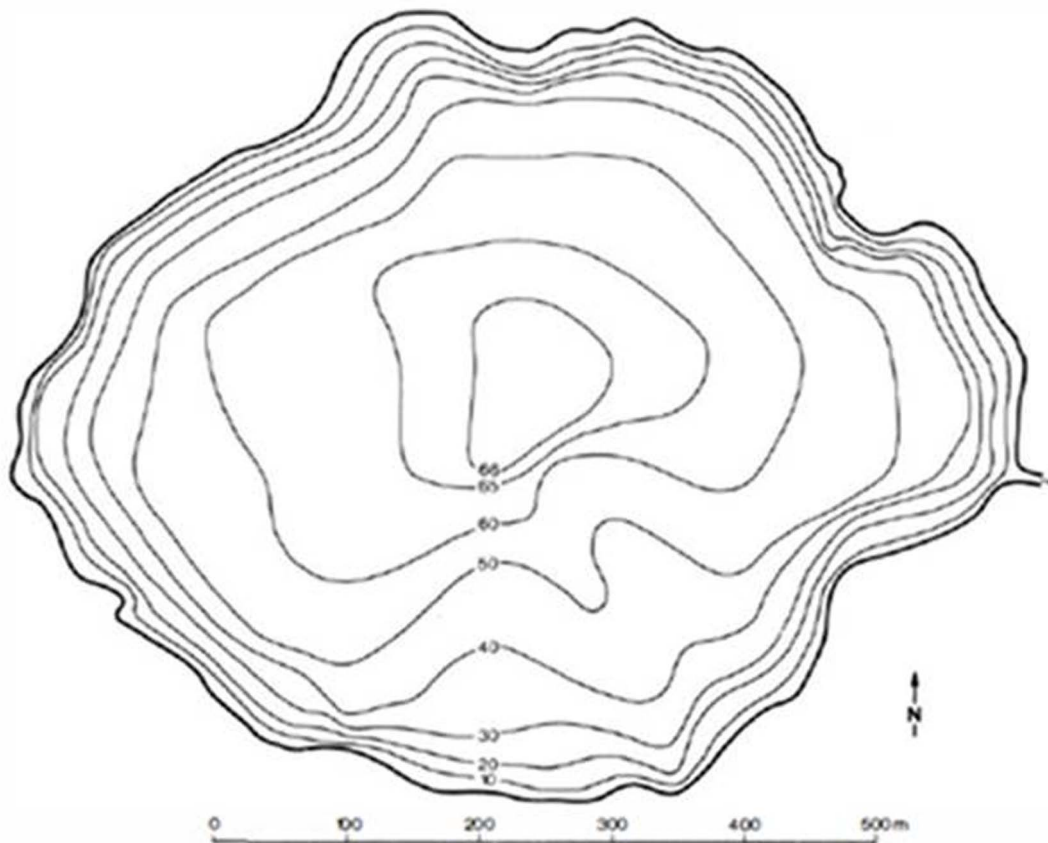doi:10.1371/journal.pone.0102456.g002

Figure 3. Panoramic view and bathymetric map of Lake Río Cuarto (modified after Göcke *et al.* [25]).

Table 1. Depth (m), temperatures (°C), pH, Eh (mV), EC (μS cm^{-1}), chemical composition, TDS (total dissolved solids), δD-H$_2$O and δ^{18}O-H$_2$O (expressed as ‰ V-SMOW) and δ^{13}C$_{TDIC}$ and δ^{13}C$_{TDICcalc}$ (expressed as ‰ V-PDB) values of water samples collected.

Lake	depth	date	T	pH	Eh	HCO$_3^-$	F$^-$	Cl$^-$	NO$_3^-$	SO$_4^{2-}$	Ca^{2+}	Mg^{2+}	Na$^+$	K$^+$	NH$_4^+$	Fe$_{tot}$	Mn	TDS	δD-H$_2$O	δ^{18}O-H$_2$O	δ^{13}C$_{TDIC}$	δ^{13}C$_{TDICcalc}$
Hule	0	March-10	24.1	7.0	11	42	0.04	1.2	0.05	2.0	7.0	2.3	2.8	1.5	0.01	0.09	0.003	60	−20.3	−3.8	n.a.	n.a.
	5	March-10	21.8	6.5	33	42	0.04	1.9	0.04	2.1	7.4	2.6	3.1	1.7	0.01	n.a.	n.a.	61	n.a.	n.a.	n.a.	n.a.
	10	March-10	21.1	6.3	23	46	0.04	1.2	0.09	2.2	7.2	2.5	3.5	1.5	0.2	0.03	0.92	66	−19.8	−3.7	−11.8	n.a.
	15	March-10	20.9	6.5	−170	60	0.03	1.8	0.07	1.4	7.5	2.8	3.4	1.5	0.4	n.a.	n.a.	79	−n.a.	n.a.	n.a.	n.a.
	23	March-10	20.8	6.6	−227	61	0.04	1.2	0.07	1.9	8.2	2.7	3.6	1.5	0.3	8.0	0.78	90	−22.5	−3.9	−14.3	−12.2
Rio Cuarto	0	March-10	27.9	7.5	166	85	0.05	1.8	0.4	1.1	12	5.1	5.7	2.7	1.9	0.02	0.004	116	−20.3	−3.3	−8.3	n.a.
	10	March-10	24.7	6.8	−191	92	0.04	1.9	0.6	0.88	13	5.1	5.5	2.7	2.0	3.4	0.27	127	−19.7	−3.4	−7.9	n.a.
	20	March-10	24.7	6.8	−215	93	0.04	1.7	0.1	0.91	13	5.1	5.5	2.7	2.1	n.a.	n.a.	124	n.a.	n.a.	−7.8	−7.8
	30	March-10	24.7	6.8	−230	93	0.04	1.9	0.03	1.1	13	4.9	5.5	2.7	2.1	n.a.	n.a.	124	n.a.	n.a.	−8.6	−8.8
	40	March-10	24.6	6.8	−243	103	0.05	2.1	0.03	0.95	14	5.0	5.5	2.8	2.4	3.6	0.27	140	−22.2	−3.4	−8.4	−8.9
	50	March-10	24.7	6.6	−239	105	0.05	1.8	0.03	0.67	13	5.1	5.6	2.8	3.3	5.4	0.36	143	−22.6	−3.5	−5.1	−7.3
	60	March-10	24.7	6.5	−245	163	0.06	1.8	0.08	0.51	14	5.6	5.9	3.3	9.0	15	0.63	219	−24.5	−3.7	−3.7	−2.0
	67	March-10	24.7	6.6	−246	179	0.05	1.9	0.09	0.42	15	6.0	6.1	3.5	11	22	0.66	246	−23.6	−3.6	−5.2	−1.6

Ion contents and TDS are in mg L^{-1}. n.a.: not analyzed; n.d.: not detected.
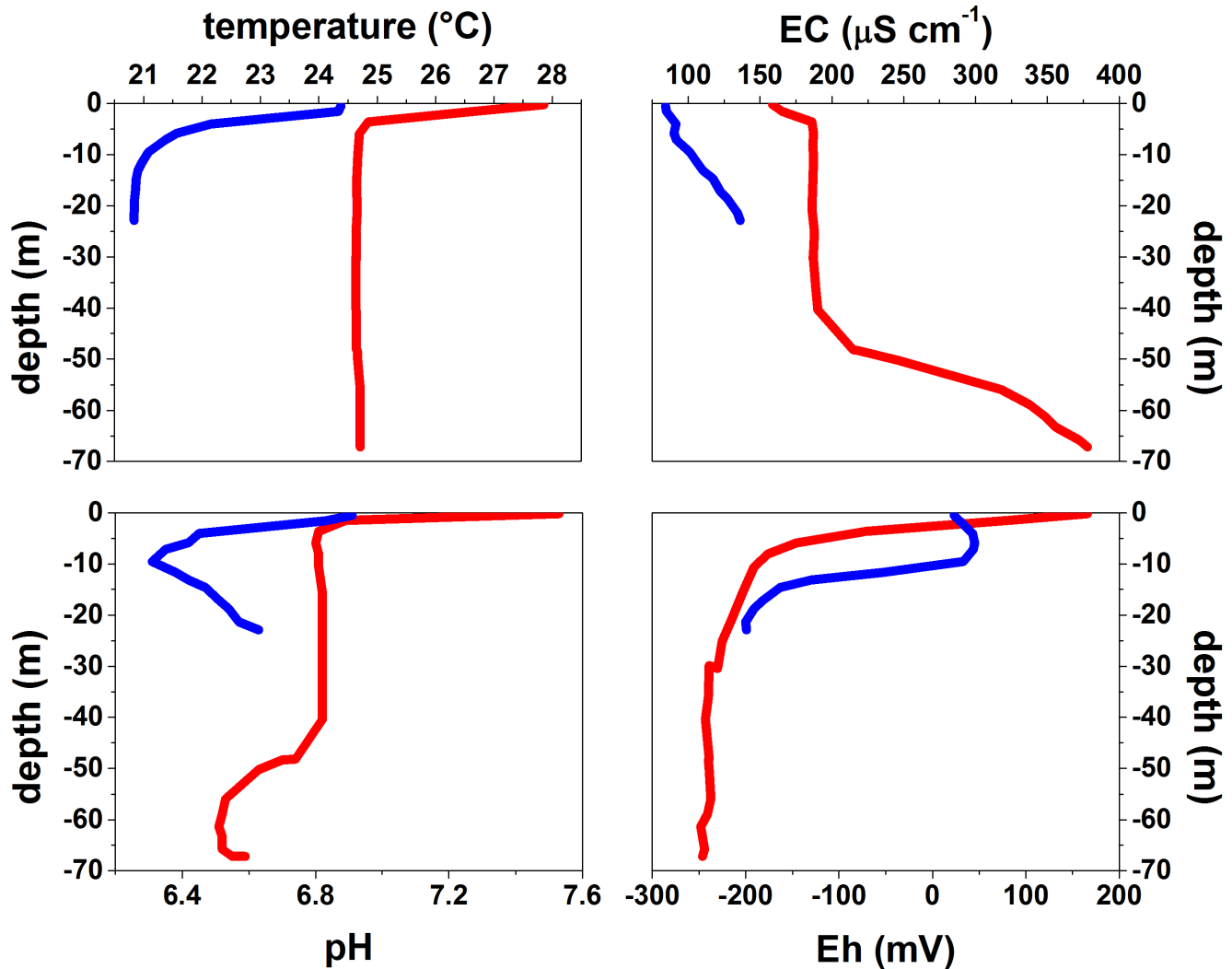doi:10.1371/journal.pone.0102456.t001

Figure 4. Vertical profiles of temperature (°C, a), electrical conductivity (EC, in µS cm^{-1}, b), pH (c), and redox potential (Eh, in mV, d) in Lake Hule (blue line) and Lake Río Cuarto (red line).
doi:10.1371/journal.pone.0102456.g004

hydrogen [41]. The analytical uncertainties were ±0.08‰ and ±1‰ for $\delta^{18}O$ and δD values, respectively.

The $^{13}C/^{12}C$ ratios of TDIC (expressed as $\delta^{13}C_{TDIC}$ ‰ vs. V-PDB) at selected depths were determined on CO_2 produced by reaction of 3 mL of water with 2 mL of anhydrous phosphoric acid in vacuum [42] using a Finningan Delta Plus XL mass spectrometer. The recovered CO_2 was analyzed after a two-step extraction and purification procedures of the gas mixtures by using liquid N_2 and a solid-liquid mixture of liquid N_2 and trichloro-ethylene [43,44]. The analytical uncertainty was ±0.05 ‰.

Dissolved gas composition was calculated using i) the composition of the gas phase stored in the headspace of the sampling glass flasks, ii) the gas pressure in the flask headspace, iii) the headspace volume, and iv) the solubility coefficients in water of each gas compound [45]. The inorganic gas compounds hosted in the flask headspace (CO_2, N_2, CH_4, Ar, O_2, Ne, H_2 and He) were determined using a gas-chromatograph (Shimadzu 15a) equipped with a Thermal Conductivity Detector (TCD). Methane was analyzed with a Shimadzu 14a gas-chromatograph equipped with a Flame Ionization Detector (FID). The analytical error for dissolved gas analysis was ≤5%.

The analysis of the $^{13}C/^{12}C$ ratios of CO_2 (expressed as $\delta^{13}C$-CO_2 ‰ vs. V-PDB) stored in the flask headspace ($\delta^{13}C$-CO_{2STRIP}) of selected samples was carried out with a Finningan Delta S mass spectrometer after standard extraction and purification procedures of the gas mixtures [43,44]. Internal (Carrara and San Vincenzo marbles) and international (NBS18 and NBS19) standards were used for the estimation of external precision. The analytical uncertainty was ±0.05‰. The $^{13}C/^{12}C$ ratio of dissolved CO_2 ($\delta^{13}C$-CO_2) was calculated from the $\delta^{13}C$-CO_{2STRIP} values using the ε_1 factor for gas-water isotope equilibrium proposed by Zhang *et al.* [46], as follows:

$$\varepsilon_1 = \delta^{13}C - CO_2 - \delta^{13}C - CO_{2STRIP} = (0.0049 \times T) - 1.31 \quad (1)$$

The analysis of the $^{13}C/^{12}C$ and $^2H/^1H$ ratios of dissolved CH_4 (expressed as $\delta^{13}C$-CH_4 ‰ vs. V-PDB and δD-CH_4 ‰ vs. V-SMOW, respectively) of selected samples was carried out by mass spectrometry (Varian MAT 250) according to the procedure and the sample preparation described by Schoell [47]. The analytical uncertainty was ±0.15‰.
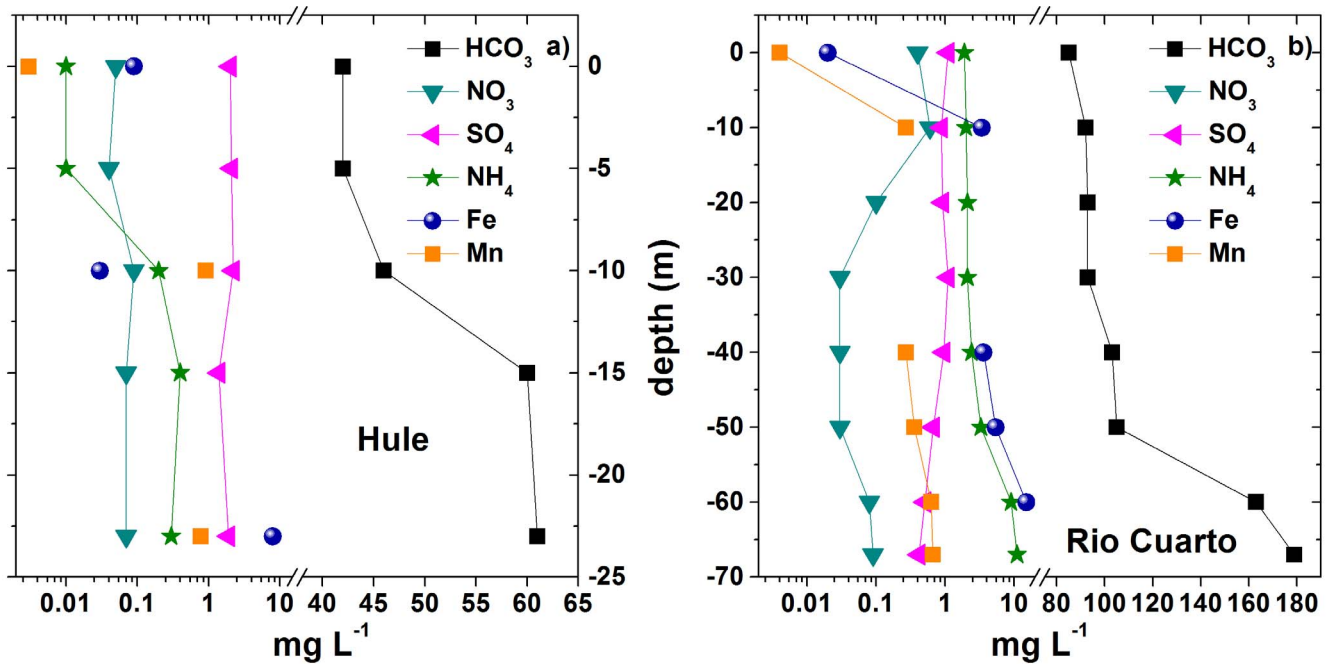
Figure 5. Vertical profiles (in mg L^{-1}) of HCO$_3$$^-$, NO$_3$$^-$, SO$_4$$^{2-}$, NH$_4$$^+$, Fe$_{tot}$ and Mn in Lake Hule (a) and Lake Río Cuarto (b).
doi:10.1371/journal.pone.0102456.g005

The ^{3}He/^{4}He ratios, expressed as R/Ra values, where R is the ^{3}He/^{4}He isotopic ratio in gas samples and Ra is that of the air equal to 1.39×10^{-6} [48,49], were determined in selected gas samples stored in the sampling flask headspace at the INGV laboratories of Palermo, using the method described in Inguaggiato and Rizzo [50]. The R/Ra values were corrected for air contamination on the basis of measured He/Ne ratios. The analytical uncertainty was ±0.3%.

3.4 Microbiological analysis

DNA extraction for the analysis of microbial populations was performed according to the protocol reported by Mapelli et al. [51] and quantified by NanoDrop 1000 spectrophotometer (Thermo Scientific, Waltham, MA). 16S rRNA gene was amplified in PCR reactions using universal primers for bacteria with GC-clamp as described in Marasco et al. [52]. Denaturing Gradient Gel Electrophoresis (DGGE), applied to the bacterial 16S rRNA gene amplified from the total water metagenome, was performed by loading DGGE-PCR products (~150 ng) in a 0.5 mm polyacrylamide gel (7% [w/v] acrylamide-bisacrylamide, 37.5:1) containing 40 to 55% urea-formamide denaturing gradient, where 100% denaturant corresponds to 7 M urea and 40% [vol/vol] formamide [52]. DGGE profiles were analyzed by using Image J software (available at http://rsb.info.nih.gov/ij/) and cluster analysis was performed using Microsoft Excel XLSTAT software (Addinsoft Inc., New York, NY, USA). DGGE bands were excised from the gel, eluted in water, PCR amplified and sequenced as previously described [52]. The partial 16S rRNA gene sequences obtained from the excised DGGE bands were edited in Chromas lite 2.01 (http://www.technelysium.com.au) and subjected to BLAST search (http://blast.ncbi.nlm.nih.gov/Blast.cgi). The nucleotide sequences were deposited in the EMBL public database under the accession numbers HF930552-HF930593. To test the presence of bacteria involved in anaerobic ammonium oxidation (anammox), the functional gene *hzsA* was amplified using primers hzsA_526F and hzsA_1857R as previously reported [53].

454 pyrosequencing assays were performed by using universal-bacterial primers targeting the variable regions of the 16S rRNA, V1–V3 (27 F mod 5′ – AGRGTTTGATCMTGGCTCAG – 3′; 519 R mod bio 5′ - GTNTTACNGCGGCKGCTG - 3′), amplifying a fragment of approximately 400 bp, and 16S rRNA archaeal primers arch344F (5′ - ACGGGGYGCAGCAGGCG-CGA – 3′) and arch915R (5′ - GTGCTCCCCCGCCAATTCCT -3′). The amplified 16S rRNA regions contained enough nucleotide variability to be useful in identification of bacterial and archaeal species [54,55]. PCR reactions and next generation 454 pyrosequencing were performed at MR DNA laboratories (Shallowater, TX – U.S.A.). A first quality filtering was applied, removing all the sequences that were shorter than 300 bp, longer than 500 bp or with an average quality score under 25. All original and non-chimeric 454 sequences are archived at EBI European Read Archive. The high-quality 16S rRNA gene sequences obtained by 454 pyrosequencing were analysed using QIIME [56]. The sequences were clustered into operational taxonomic units based on a threshold of 97% (OTU$_{97}$) sequence identity, using uclust [57] and one sequence for each OTU$_{97}$, as representative, was aligned to Greengenes (http://greengenes.lbl.gov/) using PyNast [56]. Sequence identification was conducted using Ribosomal Database Project classifier [58], with default parameters. For each sample rarefaction curves of the observed species and of Shannon index were estimated in order to analyse the species sampling coverage. The OTU$_{97}$ diversity within and between sample/s (respectively alpha and beta diversity) was estimated using QIME workflow script alpha_rarefaction.py. Shannon diversity index was calculated by PAST software [59]. Library coverage was calculated for each library using the equation C = [1– (n1/N)] ×100, where n1 is the number of singleton OTU$_{97}$, and N is the total number of reads in the library. To remove noise from the data, including potential rare contaminants, OTU$_{97}$ not meeting the criterion of being present at least 0.1% of the total number of reads were removed.

Table 2. Trace elements composition of water samples collected.

Lake	depth	Al	As	B	Ba	Cd	Co	Cr	Cs	Cu	Li	Mo	Ni	Pb	Rb	Sb	Se	Sr	Th	Ti	U	V	Zn
Hule	0	5.4	0.11	5.0	5.1	0.04	<0.05	<0.05	0.04	0.25	0.11	0.11	0.66	0.04	4.6	0.01	0.03	69	<0.02	0.31	<0.02	0.88	3.3
	5	n.a.	n.a.	n.a.	n.a.	n.a.	n.a.	n.a.	n.a.	n.a.	n.a.	n.a.	n.a.	n.a.	n.a.	n.a.	n.a.	n.a.	n.a.	n.a.	n.a.	n.a.	n.a.
	10	5.0	0.12	4.5	9.0	0.08	0.61	<0.05	0.05	0.12	0.11	0.12	0.79	0.04	4.9	0.01	0.02	81	<0.02	0.30	<0.02	0.40	4.4
	15	n.a.	n.a.	n.a.	n.a.	n.a.	n.a.	n.a.	n.a.	n.a.	n.a.	n.a.	n.a.	n.a.	n.a.	n.a.	n.a.	n.a.	n.a.	n.a.	n.a.	n.a.	n.a.
	23	12	0.54	4.5	15	<0.01	1.4	<0.05	0.06	<0.05	0.11	0.16	1.0	0.03	5.4	0.01	0.03	100	<0.02	0.47	<0.02	1.8	1.5
Rio Cuarto	0	11	0.25	8.8	6.8	0.08	0.16	0.05	0.08	0.38	0.21	0.77	1.0	0.12	8.1	0.17	0.06	118	<0.02	0.66	0.02	0.76	5.1
	10	7.4	0.21	7.9	20	0.04	0.55	<0.05	0.08	0.10	0.15	0.22	2.8	0.06	8.0	0.03	0.02	115	<0.02	0.44	<0.02	1.0	3.1
	20	n.a.	n.a.	n.a.	n.a.	n.a.	n.a.	n.a.	n.a.	n.a.	n.a.	n.a.	n.a.	n.a.	n.a.	n.a.	n.a.	n.a.	n.a.	n.a.	n.a.	n.a.	n.a.
	30	n.a.	n.a.	n.a.	n.a.	n.a.	n.a.	n.a.	n.a.	n.a.	n.a.	n.a.	n.a.	n.a.	n.a.	n.a.	n.a.	n.a.	n.a.	n.a.	n.a.	n.a.	n.a.
	40	11	0.21	7.9	22	0.01	0.56	0.06	0.08	0.10	0.14	0.14	1.4	0.15	8.0	0.02	0.02	115	<0.02	0.52	<0.02	1.1	2.8
	50	6.1	0.23	9.1	34	0.01	0.75	<0.05	0.09	0.05	0.15	0.12	1.7	0.04	9.0	0.02	0.02	130	<0.02	0.50	<0.02	1.2	4.5
	60	8.1	0.38	9.6	91	<0.01	1.6	<0.05	0.12	0.10	0.11	0.05	3.1	0.03	10	0.01	0.03	149	<0.02	0.83	<0.02	1.6	3.3
	67	30	0.45	9.3	108	0.02	1.8	0.06	0.12	1.0	0.08	<0.05	3.8	0.22	9.9	0.02	0.04	145	<0.02	1.30	<0.02	2.2	8.4

Chemical concentrations are in $\mu g\ L^{-1}$. n.a.: not analyzed.
doi:10.1371/journal.pone.0102456.t002

Results

4.1 Vertical profiles of temperature, EC, pH and Eh

Temperature, EC, pH, and Eh along the vertical profiles of the lakes are shown in Tab. 1 and Fig. 4. Both Hule and Río Cuarto lakes showed relatively high temperature at the surface (24.1 and 27.9°C, respectively), and a thermocline at shallow depths (starting from -2.5 and -5 m, respectively), with minimum temperatures of 20.8 and 24.6°C, respectively, at the lake bottoms (Fig. 4a). The temperature profiles were consistent with those reported in previous studies [17,18,23,24,25,32,60], except those of the epilimnion, likely because present and past measurements were carried out in different periods of the year. Lake Hule did not show a clear chemocline, as shown by the EC values that almost constantly increased (from 84 to 140 $\mu S\ cm^{-1}$) with depth (Fig. 4b). Conversely, Lake Río Cuarto showed two chemoclines: the first one (from 159 to 186 $\mu S\ cm^{-1}$) near the surface and the second one (from 190 to 378 $\mu S\ cm^{-1}$) between -40 and -67 m depth. The vertical profile of pH values at Lake Hule exhibited a sharp decrease from 6.9 to 6.3 between the depths of 0 m and 10 m, and an opposite trend below this depth, where pH rose from 6.3 to 6.6 (Fig. 4c). At Lake Río Cuarto the pH values decreased in the shallower water strata (from 7.5 to 6.8) and from -40 to -60 m depth (from 6.8 to 6.5), and slightly increased (up to 6.6) at the lake bottom (Fig. 4c). Eh values at Lake Hule (Fig. 4d) showed a sharp decrease between -10 and -15 m (from 33 to -163 mV) and reached the minimum values at lake bottom (-200 mV), whereas at Lake Río Cuarto it strongly decreased (from $+166$ at surface to -191 mV) at the depth of 10 m displaying the lowest value (-246 mV) at the lake bottom.

4.2 Chemical and isotopic composition of water samples

Both lakes showed low TDS values (up to 90 and 246 mg L^{-1}, respectively, at lakes bottom) and a Ca^{2+}-HCO_3^- composition (Tab. 1). Concentrations of HCO_3^-, NH_4^+, Fe_{tot} and Mn (Fig. 5a–b) tended to increase towards the two lakes bottom (up to 61 and 179 mg L^{-1}, 0.3 and 11 mg L^{-1}, 8 and 22 mg L^{-1}, 0.9 and 0.7 mg L^{-1} in Hule and Río Cuarto, respectively), whilst oxidized nutrients NO_3^- and SO_4^{2-}, typical electron acceptors in anaerobic environments, showed an opposite behaviour in Lake Río Cuarto, decreasing to 0.03 and 0.4 mg L^{-1}, respectively (Fig. 5b). On the contrary, F^-, Cl^-, Ca^{2+}, Mg^{2+}, Na^+, K^+ and, only in Lake Hule, NO_3^- and SO_4^{2-}, did not display specific vertical trends along the lakes water column.

The δD-H_2O values in Hule and Río Cuarto lakes ranged from -26.5 to -20.5 ‰ and -24.4 to -19.7 ‰ V-SMOW, respectively, while those of $\delta^{18}O$-H_2O varied from -4.7 to -4.6 ‰ and from -4.5 to -4.0 ‰ V-SMOW, respectively (Tab. 1). The $\delta^{13}C_{TDIC}$ values were between -14.3 and -11.8 ‰ and -8.6 to -3.7 ‰ V-PDB, in Hule and Río Cuarto, respectively.

Trace element composition did not differ significantly between the two lakes. The most abundant trace elements ($>4\ \mu g\ L^{-1}$) along Hule and Río Cuarto vertical profiles were Al, B, Ba, Rb, Sr and Zn. The maximum concentrations of Co, Cu, Ni, Ti and V ($<2.2\ \mu g\ L^{-1}$) were observed at the bottom layer of Lake Río Cuarto (-67 m) and the other measured trace elements (As, Cd, Cr, Cs, Li, Mo, Pb, Sb, Se, Th, U) were all $<1\ \mu g\ L^{-1}$ (Tab. 2). In terms of vertical distribution, those trace elements that clearly increased towards both lakes bottom were Al, As, Ba, Co, Ni, Sr, Ti and V (Tab. 2), whilst Mo concentrations showed a decrease with depth only in Lake Río Cuarto.

Table 3. Chemical composition (µmol L^{-1}) and total pressure (pTOT; in atm) of dissolved gases (CO_2, N_2, CH_4, Ar, O_2, Ne, H_2 and He) and $\delta^{13}C$-CO_2 (expressed as ‰ V-PDB), $\delta^{13}C$-CH_4 (expressed as ‰ V-PDB), δD-CH_4 (expressed as ‰ V-SMOW) and R/Ra values of gas samples collected.

lake	depth	CO_2	N_2	CH_4	Ar	O_2	Ne	H_2	He	pTOT	$\delta^{13}C$-CO_2	$\delta^{13}C$-CH_4	δD-CH_4	R/Ra	He/Ne
Hule	0	n.a.	n.a.	n.a.	n.a.	n.a.	n.a.	n.a.	n.a.	n.a.	n.a.	n.a.	n.a.	n.a.	n.a.
	5	29	520	n.d.	13	160	0.006	0.007	n.d.	0.88	n.a.	n.a.	n.a.	n.a.	n.d.
	10	191	537	1.7	12	n.d.	0.005	0.005	0.005	0.79	n.a.	n.a.	n.a.	n.a.	1.0
	15	257	552	66	13	n.d.	0.006	0.01	0.008	0.85	n.a.	n.a.	n.a.	n.a.	1.4
	23	1090	618	232	15	n.d.	0.008	0.01	0.03	1.1	−16.2	−62.5	−159	0.95	4.1
Rio Cuarto	0	n.a.	n.a.	n.a.	n.a.	n.a.	n.a.	n.a.	n.a.	n.a.	n.a.	n.a.	n.a.	n.a.	n.a.
	10	239	528	73	12	0.33	0.006	0.01	n.d.	0.87	n.a.	n.a.	n.a.	n.a.	n.d.
	20	357	524	206	13	n.d.	0.007	0.02	n.d.	0.96	−14.3	−60.7	−233	n.a.	n.d.
	30	751	559	546	13	n.d.	0.007	0.02	0.31	1.3	−14.2	−61.9	−239	n.a.	45
	40	1045	576	746	14	n.d.	0.007	0.02	0.05	1.4	−13.9	−63.8	−241	n.a.	7.6
	50	1450	522	1080	13	n.d.	0.007	0.03	0.09	1.6	−11.6	−72.3	−250	1.15	13
	60	2090	538	2435	13	n.d.	0.006	0.05	0.25	2.6	−6.5	−74.8	−248	n.a.	39
	67	1790	532	2830	13	n.d.	0.007	0.04	0.34	2.9	−6.6	−77.2	−251	1.09	49

Dissolved gas concentrations are in µmol L^{-1}. n.a.: not analyzed; n.d.: not detected.
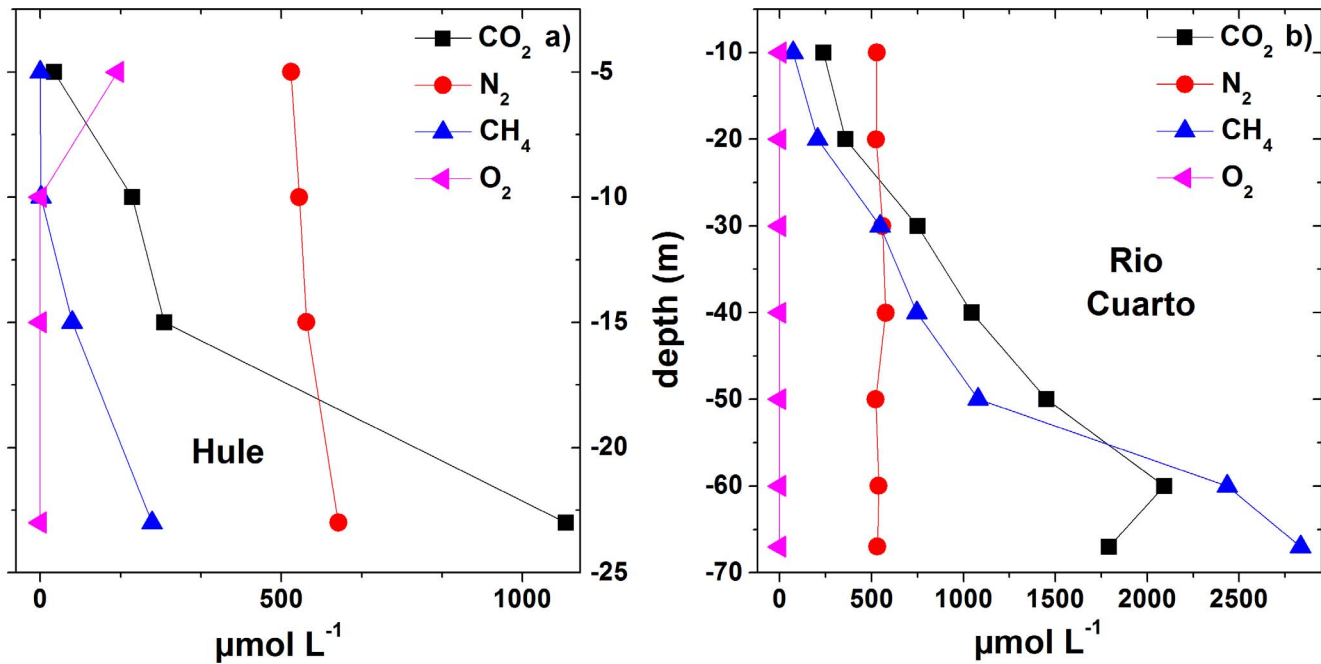doi:10.1371/journal.pone.0102456.t003

Figure 6. Vertical profiles (in μmol L^{-1}) of CO$_2$, N$_2$, CH$_4$ and O$_2$ in Lake Hule (a) and Lake Río Cuarto (b).
doi:10.1371/journal.pone.0102456.g006

4.3 Chemical and isotopic composition of dissolved gases

Molecular nitrogen was the most abundant dissolved gas in the shallow portion of the two lakes (down to the depths of −15 m and −20 m at Lake Hule and Lake Río Cuarto, respectively; Tab. 3). At lower depths CO$_2$ dominated the gas composition (up to 1090 and 2090 μmol L^{-1} at Lake Hule and Lake Río Cuarto, respectively), except at the bottom of Lake Río Cuarto (Fig. 6a–b) where CH$_4$ concentrations up to 2830 μmol L^{-1} were measured. O$_2$ is not present below −10 m depth at Hule and Río Cuarto, defining a clear anaerobic zone (Fig. 6a–b). Ar and Ne did not vary significantly with depth, whereas H$_2$ and He concentrations increased with depth in both lakes (up to 0.01 and 0.03 μmol L^{-1} and to 0.04 and 0.3 μmol L^{-1} in Hule and Río Cuarto, respectively; Tab. 3). It is noteworthy to point out that He was an order of magnitude more abundant at Río Cuarto than at Hule. The maximum total pressure (pTOT; Tab. 3) value of dissolved gases was measured at the bottom of Lake Río Cuarto (2.9 atm), whereas pTOT in Lake Hule ranged from 0.79 to 1.1 atm.

The δ^{13}C-CO$_2$ value at the bottom of Lake Hule was −16.2 ‰ V-PDB (Tab. 3). At Lake Río Cuarto, the δ^{13}C-CO$_2$ values showed an increase with depth, ranging from −14.3 at −20 m to −6.5 ‰ V-PDB at the lake bottom. No specific trends were recognized in the epilimnion (Fig. 7). The δ^{13}C-CH$_4$ values, basically characterized by the same interval (from −77.2 to −60.7 ‰ V-PDB) in both lakes, showed a rapid decrease in the Río Cuarto hypolimnion. The δD-CH$_4$ values of Lake Río Cuarto were significantly more negative (from −251 to −233 ‰ V-SMOW) when compared to that of Lake Hule bottom (−159 ‰ V-SMOW; Tab. 3). The R/Ra values, corrected for the presence of atmospheric helium [61], were 0.95 in Lake Hule (lake bottom) and 1.15 and 1.09 in Lake Río Cuarto (at −50 and −67 m depth, respectively; Tab. 3).

4.4 Prokaryotic diversity along the water column

Phylogenetic analyses of 16S rRNA DGGE derived sequences (Fig. 8a–b) allowed to detect 7 phyla within the bacterial communities and to identify the prevalent taxonomic groups colonizing the Hule and Río Cuarto lakes at different depths (Tab. 4). Overall, the sequences were related to uncultured unclassified bacteria previously described in aquatic environments, mainly represented by freshwater of lacustrine origin.

At Lake Hule a clear shift in taxa distribution was evaluated, corresponding to the transition at ~10 m depth of the redox potential from positive to negative. The lake epilimnion was mainly colonized by aerobic heterotrophic Bacteroidetes and Betaproteobacteric while deeper anoxic layers (>10 m depth; Fig. 4d) were inhabited by bacteria belonging to the phylum Chlorobi, comprising anaerobic photoautotrophic bacteria (*Chlorobium clathratiforme* and *Ignavibacterium album*). Bacteroidetes and Betaproteobacteria phyla were also the main components of the bacterial community in Lake Río Cuarto. In this lake the shallower portion (down to the depth of 40 m) was colonized by Cyanobacteria affiliated to the genera *Synechococcus*, *Merismopedia* and *Cyanobium*. Differently from Lake Hule, the more uniform composition of the bacterial community in Lake Río Cuarto can be related to the homogeneity of the redox conditions along the water column, which is negative in all the analyzed layers except at the lake surface (Fig. 4d).

The results of DGGE analysis were taken into account to select a sub-set of samples to gain a deeper insight into the microbiome structure by massive pyrosequencing of bacterial and archaeal 16S rRNA libraries. This high-throughput analysis was applied to 3 samples for each lake (0, 10, 15 m depth from Lake Hule, named H0, H10 and H15, and 30, 50, 60 m depth from Lake Río Cuarto, named RC30, RC50 and RC60). Unfortunately, any archaeal library could not be obtained from sample H0. The number of final reads varied among the samples, similarly to the OTU$_{97}$ number, nonetheless a significant coverage of bacterial and archaeal diversity was reached in all the samples (Tab. 5). The
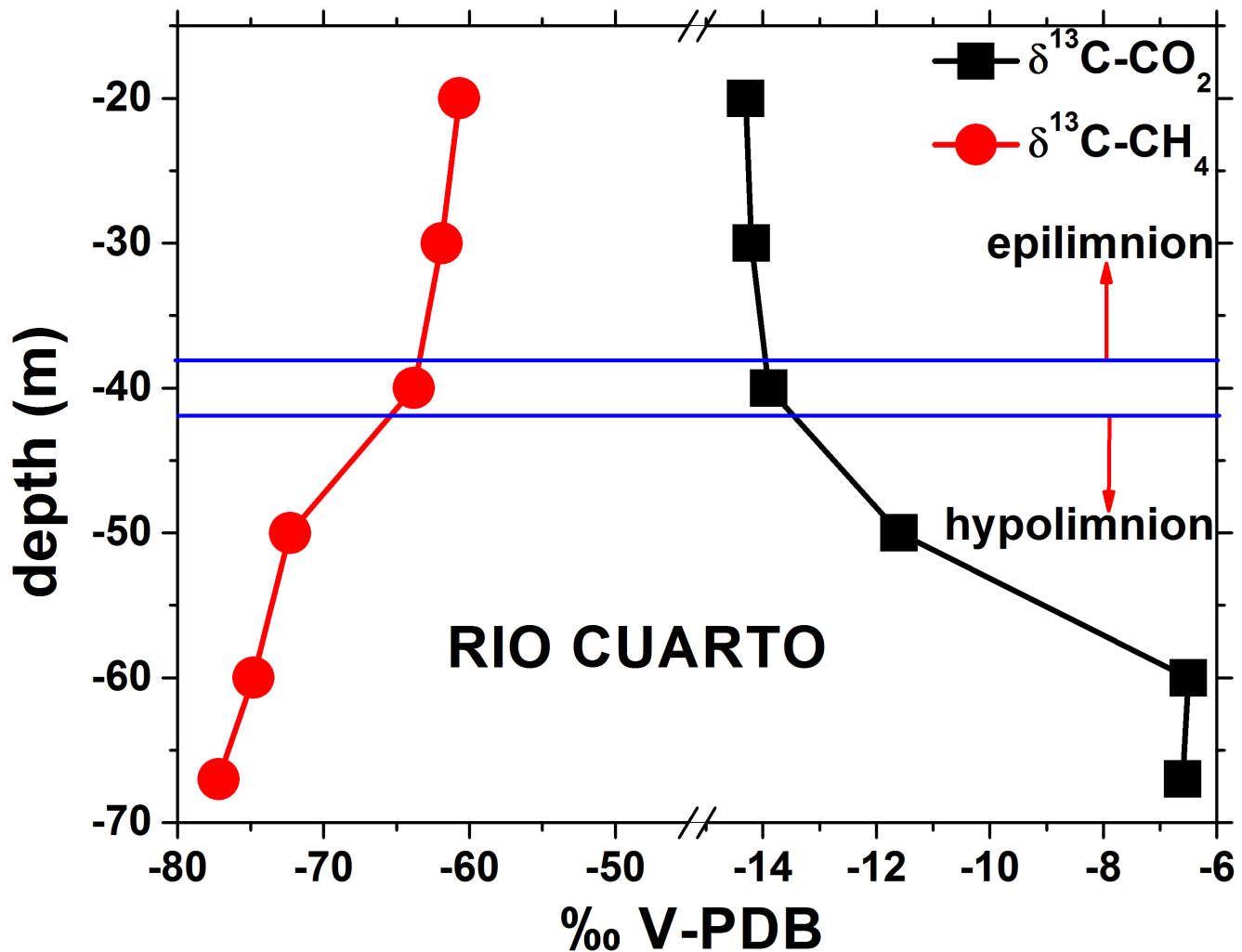
Figure 7. Vertical distribution of δ^{13}C-CO$_2$ and δ^{13}C-CH$_4$ of Lake Río Cuarto. See the text for further details.
doi:10.1371/journal.pone.0102456.g007

number of OTU$_{97}$ present in the archaeal communities was constant along the water column of Lake Rio Cuarto, while in Lake Hule a significant increase was observed with depth (Tab. 5). In all the samples, Proteobacteria were the most abundant bacterial phylum, with the exception of the water samples collected from Lake Rio Cuarto at 50 and 60 m depths (RC50 and RC60) where Cyanobacteria and Chloroflexi were the prevalent phyla, respectively (Tab. 6). Cyanobacteria were also present at high percentage (29.4%) in the oxic surface water sample in lake Hule (Tab. 6). The phylum Chlorobi was widespread in both the lakes in all the samples characterized by negative Eh values, with significant prevalence at 10 and 15 m depth in Lake Hule (18.5 and 17.6%, respectively). Among Proteobacteria, the Epsilon-subgroup was a minor community component in both lakes and Deltaproteobacteria were more abundant in Río Cuarto, especially in the deeper layers (Tab. 6). Alpha- and Gamma-proteobacteria were differently distributed in the two lakes. The latter were particularly abundant in shallower Hule layers (H10 and H15), while the former were present at high percentages throughout the whole Hule water column (Tab. 6). The class Betaproteobacteria, mainly represented by the *Comamonadaceae* and *Methylophilaceae* families, was abundant at all depths in both the lakes (Tab. 6). In Lake Hule between 12.9 and

22.8% of the bacterial community was represented by sequences belonging to the ACK-M1 cluster of the order Actinomycetales, whose presence in lacustrine habitats was previously reported (Tab. 6) [62]. At the oxic-anoxic interfaces, anaerobic ammonium oxidation (anammox) was indicated as an autotrophic denitrification metabolism co-responsible of nitrogen loss from water environments [63]. The research of bacterial taxa known to be responsible of anammox reaction was performed by amplifying with specific primers the functional gene *hzsA*, encoding for hydrazine synthase and recently proposed as an anammox phylomarker [53]. The PCR amplification showed negative results, confirming that anammox populations are absent at Hule and Rio Cuarto lakes.

As far as the archaeal community is concerned, Euryarchaeota were the most abundant phylum in Lake Rio Cuarto (up to 99%). Methanomicrobia were the most abundant class within this phylum, encompassing in particular the orders *Methanomicrobiales* and *Methanosarcinales* (Tab. 7). Lake Hule showed a different archaeal community, being dominated by Parvarchea and Micrarchaea, with significant concentrations of Crenarchaeota (8.1 and 13.7% at 10 and 15 m depth, respectively), and a minor percentage of Methanomicrobia and unknown taxa (Tab. 7).
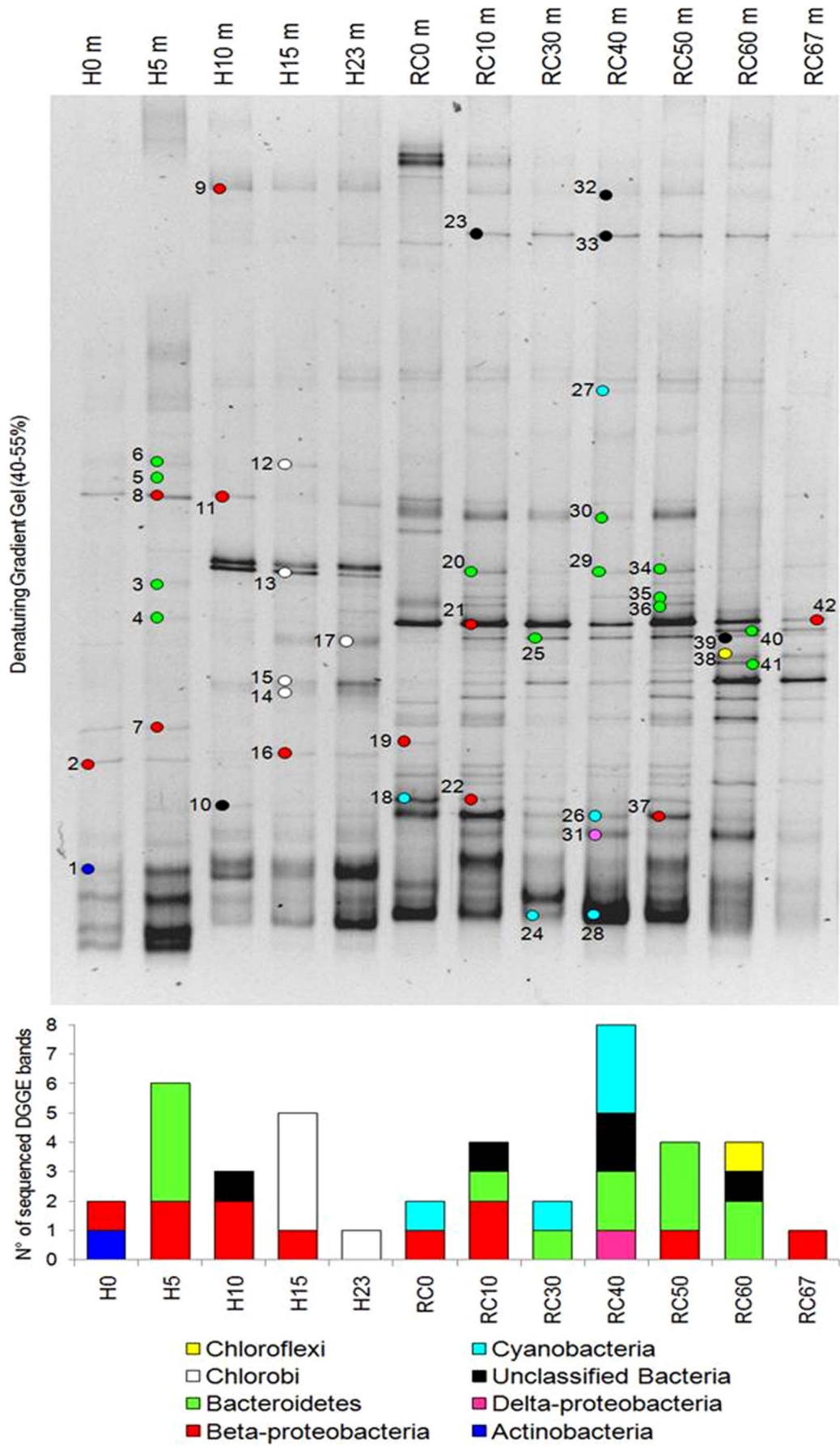
Figure 8. DGGE analysis performed on the bacterial 16S rRNA gene, showing the structure of the bacterial community inhabiting freshwater samples collected from the Hule and Río Cuarto lakes (a); taxonomic identification of bacterial 16S rRNA sequences excised from DGGE bands cut from the Lake Hule and Río Cuarto water profiles (b).
doi:10.1371/journal.pone.0102456.g008

Discussion

5.1 Processes controlling the water chemistry

Water isotopes can provide notable information on physical-chemical processes affecting the chemistry of volcanic lakes, such as evaporation, water-rock interaction and hydrothermal/meteoric inputs [64]. As shown in Fig. 9, water samples plot near the Global Meteoric Water Line (GMWL) [65] and the Costa Rica Surface Water Line [66], indicated that in both lakes the main water source is meteoric, consistently with their $Ca^{2+}(Mg^{2+})$-HCO_3^- composition, which is typical for superficial waters and shallow aquifers worldwide [67]. Both lakes show a slight D- and ^{18}O- depletion at increasing depth, likely related to evaporation affecting epilimnetic waters [64,68,69].

The parallel increases of HCO_3^- (Fig. 5) and dissolved CO_2 (Fig. 6) along the vertical profiles suggest that the behaviour of these two chemical species is controlled by the following reactions:

$$CO_2 + H_2O \rightarrow H_2CO_3 \qquad (2)$$

and

$$H_2CO_3 + H_2O \rightarrow H_3O^+ + HCO_3^- \qquad (3)$$
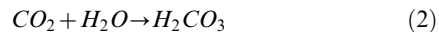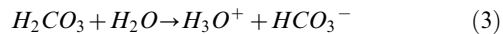
The observed weak decreases of SO_4^{2-} and NO_3^- concentrations (Fig. 5) with depth possibly result from microbial activity occurring at anaerobic conditions. The lack of free oxygen in the hypolimnion is favorable for nitrate reduction by microbial denitrification, a typical process in anoxic water bodies [70–74]. The genus *Pseudomonas* is known to include denitrifier species [75] and was retrieved at high abundance in pyrosequencing libraries in the anoxic layers of Lake Hule, constituting up to 16% of the total bacterial community (Tab. 6). In the Hule anoxic layers, 16S rRNA pyrosequencing allowed to detect additional denitrifying genera like *Sulfuricurvum, Opitutus* and *Geothrix* (Tab. 6). Sulfate reducing bacteria (SRB) of the genus *Syntrophobacter* were retrieved by 16S rRNA pyrosequencing in the deepest layers of the Río Cuarto water column (Tab. 6), and could be responsible of the weak depletion observed for SO_4^{2-} (Fig. 5b). Nevertheless, the relatively low SO_4^{2-} and NO_3^- concentrations, typical of meteoric-sourced lakes, implies that sulfate reduction and denitrification have a minor impact on the chemistry of the two lakes. The increase of NH_4^+ concentrations with depth (Fig. 5) is apparently suggesting direct NH_4^+ production within the hypolimnion via ammonification processes [76].

The increase of Fe and Mn contents in the deepest water layers can be attributed to direct production inside the bottom sediments by minerogenic processes [77–79], although their presence as solutes is limited by the formation of insoluble Fe- and Mn-hydroxides. Göcke [24] suggested that the high concentration of Fe in Lake Hule is also caused by the addiction of yellow/brownish $Fe(OH)_3$ material through the southern brooklets, which subsequently precipitates in the hypolimnion and iron is reduced to the ferrous state, as also supported by the relatively low Eh values (Fig. 4). Oxidation of hypolimnetic Fe^{2+} in the epilimnion would explain the yellow-reddish color of the shallow water layer that was occasionally observed in these lakes as a consequence of

water rollover [18,25]. Nevertheless, the red coloration observed at Lake Hule in February 1991 was likely caused by the presence of dense purple clumps or masses floating of *Merismopedia* [18], a genus belonging to the phylum Cyanobacteria that were observed by DGGE at −30 and −40 m depth in Lake Río Cuarto (Tab. 4).

As shown in the spider-diagrams of Fig. 10, where concentrations of Al, Ba, Cr, Cu, Ni, Rb, Sr, Ti and V at maximum depths for both lakes are normalized to those measured in basalt rock samples collected from the young intra-caldera cone at Laguna Hule (the only one available) [80], water-rock interactions efficiently mobilized soluble elements such as Ba, Rb and Sr, whereas Al and Ti were basically retained in the rock matrix. In particular, Cr and Ni, as well as As and Co, are possibly related to the dissolution of Mn-and Fe-oxide particles that settled through the chemocline [78,81,82]. The concentrations of dissolved V are strongly correlated with those of Fe, similarly to what observed for Mo and Mn [29,83], likely because they belong to the same mineralogical paragenesis. For what concerns the other trace elements, Cu and Zn may be related to dissolution of stable organic complexes buried in the bottom sediments [29]. Cs, Rb and B, which are strongly correlated with Li (Tab. 2), can be considered as conservative elements, likely due to the strong affinity of alkali ions and boric acid for the aqueous phase [82]. The relatively low Mo concentrations at increasing depth in Lake Río Cuarto (Tab. 2) may be related to its consumption during microbial nitrate reduction [29].

5.2 Processes governing chemical and isotopic composition of dissolved gases

5.2.1 Noble gases, N_2, O_2, and H_2. Dissolved gas species in volcanic lakes basically originate from i) external sources (e.g. atmosphere, volcanic-hydrothermal fluids) and/or ii) microbial activity occurring both in lake water and at water-sediment interface [4,14,28,84,85,86].

Dissolved Ar and Ne in lakes are related to air dissolution through the lake surface, a process that is mainly controlled by atmospheric pressure and the water temperature [87]. The inert noble gases behave inertly in any bio-geochemical process and thus along the lake water column they are affected by advection and diffusion. Accordingly, Ar and Ne concentrations in the two investigated lakes did not show significant variations with depth (Tab. 3). Conversely, O_2, which is typically consumed by aerobic microbial populations for oxidation of organic matter and reduced ionic species, rapidly decreases with depth, and was virtually absent at depths ≥5 and 10 m, in Hule and Río Cuarto lakes, respectively. It is worth noting that the N_2/Ar ratios were slightly higher than that of air saturated water (~40), suggesting the addition of N_2 from an extra-atmospheric source. This hypothesis is expected to be confirmed by $\delta^{15}N$ values that are presently not available, although the relatively high N_2/Ar ratios are apparently consistent with nitrate depletion with depth and microbial denitrification in both lakes. Consistently with the N_2 excess, the distribution of N_2 concentrations in both lakes showed significant variations with depth (Tab. 3), probably related to N_2 production and consumption by denitrifiers and nitrogen fixing prokaryotes, respectively. Microbial N_2 fixation, depending on light [88] and the presence of bio-available trace metals [89], can be carried out by heterocyst-forming species in water and in sediment pores [90–92]. *Cyanobacteria* were indeed retrieved by both DGGE and

Table 4. Phylogenetic identification of the bacterial sequences retrieved from 16S rRNA DGGE gel.

Sample	Phylum	Band	Closest relative	Acc.n°	%	Environments	Closest described specie	Acc. n°	%
Hule 0 m	Actinobacteria	1	Unc. bact.	GU127259	99	Anoxic plant reservoir	Planktophila limnetica	FJ428831	95
0 m	Betaproteobacteria	2	Massilia sp.	FJ477729	99	Soil	Massilia aerilata	EF668526	96
5 m	Betaproteobacteria	7	Unc. Betaproteobacterium	HM153624	99	Freshwater sample	Limnobacter thiooxidans	AJ289885	94
5 m	Betaproteobacteria	8	Unc. Methylophilaceae bact.	HM856563	100	Yellowstone Lake water	Methylotenera mobilis	CP001672	95
5 m	Bacteroidetes	5	Unc. Flexibacter sp.	FN668188	98	Lake Zurich water	Lishizhenia tianjinensis	EU183317	93
5 m	Bacteroidetes	3	Unc. bact.	EU803667	99	Lake Gatun water	Mucilaginibacter daejeonensis	AB267717	83
5 m	Bacteroidetes	4	Unc. bact.	JF295800	97	Soil	Pedobacter terricola	EF446147	83
5 m	Bacteroidetes	6	Unc. bact.	HM129930	98	Freshwater	Lishizhenia tianjinensis	EU183317	92
10 m	Bacteria	9	Unc. bact.	DQ642387	99	Anoxic freshwater	Chlorobium phaeovibrioides	Y08105	82
10 m	Betaproteobacteria	11	Unc. bact.	HQ653799	99	Freshwater	Methylotenera mobilis	CP001672	95
10 m	Betaproteobacteria	10	Unc. Undibacterium sp.	GU074344	99	Water sample	Undibacterium pigrum	AM397630	96
15 m	Betaproteobacteria	16	Massilia sp.	FJ477729	99	Soil	Massilia aerilata	EF668526	97
15 m	Chlorobi	12	Unc. Chlorobi bact.	FJ902335	99	Limestone sinkholes	Chlorobium clathratiforme	CP001110	96
15 m	Chlorobi	13	Unc. Chlorobi bact.	FJ902335	99	Limestone sinkholes	Chlorobium clathratiforme	CP001110	96
15 m	Chlorobi	14	Unc. bact.	HM228636	99	Riverine alluvial aquifers	Ignavibacterium album	AB478415	88
15 m	Chlorobi	15	Unc. bact.	HM228636	98	Riverine alluvial aquifers	Ignavibacterium album	AB478415	88
23 m	Chlorobi	17	Unc. bact.	HM228636	92	Riverine alluvial aquifers	Ignavibacterium album	AB478415	86
Rio Cuarto 0 m	Betaproteobacteria	19	Unc. Proteobacterium	GU074082	99	Freshwater	Burkholderia andropogonis	AB021422	95
0 m	Cyanobacteria	18	Unc. bact.	GQ091396	99	Freshwater	Synechococcus rubescens	AF317076	98
10 m	Betaproteobacteria	21	Unc. bact.	DQ060410	98	Soil enrichment culture	Methylovorus glucosotrophus	FR733702	95
10 m	Betaproteobacteria	22	Unc. bact.	GU291353	98	Tropical lakes	Sulfuritalea hydrogenivorans	AB552842	94
10 m	Bacteroidetes	20	Unc. bact.	AM409988	98	Profundal lake sediments	Owenweeksia hongkongensis	AB125062	88
10 m	Bacteria	23	Unc. Chloroflexi bact.	AB116427	93	Coastal marine sediment	Ignavibacterium album	AB478415	82
30 m	Cyanobacteria	24	Unc. Cyanobacterium	FJ844093	99	High mountain lake	Merismopedia tenuissima	AJ639891	97
30 m	Bacteroidetes	25	Unc. bact.	FJ437920	97	Green Lake water	Owenweeksia hongkongensis	AB125062	88
40 m	Bacteroidetes	29	Unc. bact.	AM409988	98	Profundal lake sediment	Solitalea koreensis	EU787448	88
40 m	Cyanobacteria	26	Unc. bact.	HQ653660	97	Shallow freshwater lake	Cyanobium gracile	AF001477	96
40 m	Cyanobacteria	27	Unc. bact.	GU305729	99	Oligotrophic lakes	Cyanobium gracile	AF001477	98
40 m	Cyanobacteria	28	Unc. bact.	FJ262922	99	Freshwater	Merismopedia tenuissima	AJ639891	97
40 m	Deltaproteobacteria	31	Unc. bact.	EF515611	97	Anaerobic bioreactor sludge	Syntrophobacter pfennigii	X82875	94
40 m	Bacteria	33	Unc. Chloroflexi bact.	AB116427	93	Coastal marine sediment	Ignavibacterium album	AB478415	83
40 m	Bacteria	32	Unc. Chlorobi bact.	GQ390242	98	Low-sulphate lake	Ignavibacterium album	AB478415	82
40 m	Bacteroidetes	30	Unc. Haliscomenobacter sp.	HM208523	99	sediment resuspension	Candidatus Aquirestis calciphila	AJ786341	99
50 m	Betaproteobacteria	37	Unc. bact.	GU291353	98	Tropical lakes	Sulfuritalea hydrogenivorans	AB552842	95
50 m	Bacteroidetes	34	Unc. bact.	AM409988	98	Profundal lake sediment	Owenweeksia hongkongensis	AB125062	88
50 m	Bacteroidetes	36	Unc. bact.	FJ612364	99	Dongping Lake Ecosystems	Sphingobacterium alimentarium	FN908502	88

Table 4. Cont.

Sample	Phylum	Band	Closest relative	Acc.n°	%	Environments	Closest described specie	Acc. n°	%
50 m	Bacteroidetes	35	Unc. bact.	FJ612364	99	Dongping Lake Ecosystems	*Sphingobacterium alimentarium*	FN908502	88
60 m	Chloroflexi	38	Unc. bact.	JF305756	97	Mature fine tailings	*Dehalogenimonas lykanthroporepellens*	CP002084	86
60 m	Bacteria	39	Unc. bact.	GQ860063	99	PCB-Spiked sediments	*Dehalogenimonas lykanthroporepellens*	CP002084	85
60 m	Bacteroidetes	40	Unc. bact.	FM956124	98	Rice field soil	*Owenweeksia hongkongensis*	AB125062	87
60 m	Bacteroidetes	41	Unc. bact.	FJ437920	97	Freshwater	*Owenweeksia hongkongensis*	AB125062	88
67 m	Betaproteobacteria	42	Unc. bact.	DQ060410	98	Soil enrichment culture	*Methylovorus glucosotrophus*	FR733702	95

The table reports the identification of the dominant bands in the PCR-DGGE fingerprinting profiles marked in Fig. 8. %: percent of identity between the DGGE band sequence and closest relative sequence in GenBank. Acc. N°: Accession number of the closest relative sequence in Genebank. Environment: environment of origin of the closest relative sequence.

doi:10.1371/journal.pone.0102456.t004

pyrosequencing in surface layers of Río Cuarto and Hule lakes (where they constitute 26% of the total bacterial community in the oxic layer H0, Tab. 6), supporting the occurrence of N_2 fixation in both the lakes.

H_2 increase with depth in the hypolimnion at Hule and Río Cuarto (Tab. 3) suggests a production of H_2 likely related to fermentation of organic matter under anaerobic conditions at the water-sediment interface. Additionally, photoreactions carried out by *Cyanobacteria*, abundantly present in the Río Cuarto deep layers and in the upper layer of the Hule water columns (Tab. 6), could be responsible of H_2 production [93–97]. Once produced at the lake bottom, H_2 can be consumed acting as electron donor for hydrogenotrophic methanogenic archaea and SRB [98–100], detected in Río Cuarto pyrosequencing libraries. Moreover, it slowly diffuses up to shallower, oxygenated layers where it can be consumed by hydrogen-oxidizing bacteria [101–104].

The presence of an extra-atmospheric source for helium can be recognized on the basis of the R/Ra values (Tab. 3), which are relatively high (up to 20 or more) for mantle gases, and as low as 0.01 in fluids from crustal sources [61]. Dissolved gas samples from Hule and Río Cuarto lakes showed R/Ra values ∼1 that, coupled with the relatively high He/Ne ratios (49 and 4.1 at Lake Rio Cuarto and Lake Hule, respectively), indicate a significant fraction of mantle He, whose uprising is likely favored by the fault system characterizing this area [18].

5.2.2 CO_2 and CH_4. CO_2 and CH_4 are the most abundant extra-atmospheric dissolved gases present in Hule and Río Cuarto lakes. As already mentioned, dissolved CO_2 controls pH values and HCO_3^- concentrations. Previous studies [17,18,20,22,23] have hypothesized that these lakes are affected by CO_2 inputs through the bottom, as supported by the presence of CO_2-rich bubbling pools and caverns or boreholes with high CO_2 concentrations characterizing this area [18,105]. A significant contribution of mantle CO_2 is indicated by the $\delta^{13}C$-CO_2 value of the dissolved gas sample collected at the maximum depth of Lake Río Cuarto (−6.6 ‰ vs. V-PDB; Tab. 3), which is in the range of mantle gases (from −8 to −4 ‰ vs. V-PDB) [106]. Although not confirmed by the $\delta^{13}C$-CO_2 values, the CO_2/CH_4 ratio measured in the dissolved gas at the bottom of Lake Hule (4.7) is too high, even higher than that of Río Cuarto bottom sample (0.63), to be ascribable to microbiological processes. This would imply that even at Lake Hule a strongly negative isotopic signature of CO_2 is externally added to the bottom waters, possibly from a CO_2-rich source deriving from oxidation of previously produced hydrocarbons.

The $\delta^{13}C$-CO_2 values at the bottom of Lake Hule (−16.2 ‰ vs. V-PDB) and at depths between −20 and −50 m in Lake Río Cuarto (as low as −14.3 ‰ vs. V-PDB; Tab. 3) were intermediate between those generated by organic matter degradation [24] and mantle degassing [107–109], indicating that along the vertical profiles of both lakes, excluding the bottom layers, biogenic processes are the most important sources of CO_2.

According to the classification proposed by Whiticar [110], the $\delta^{13}C$-CH_4 and δD-CH_4 values of the Hule and Río Cuarto lakes indicate that CH_4 has a biogenic origin (Fig. 11). The vertical profiles of the concentrations and $\delta^{13}C$ values of CO_2 and CH_4 of Lake Río Cuarto (Fig. 7) were thus produced by the combination of different processes occurring at various depths in the lake:

1) At the bottom of the lake, CO_2 inputs from a deep source likely related to the hydrothermal fluid circulation [18,111] promote methanogenic processes that have their maximum efficiency within the sediments. Methanogenesis takes place through i) CO_2 reduction and ii) degradation of organic

Table 5. Library coverage estimations and sequence diversity of 16S rRNA.

Sample	N. reads/sample	N. OTU_{97}	% Coverage*	Shannon index**
H0 Bacteria	9384	586	0.98	4.21
H10 Bacteria	11115	615	0.98	4.21
H15 Bacteria	15872	1260	0.97	4.98
RC30 Bacteria	32932	3017	0.95	4.60
RC50 Bacteria	13291	1609	0.94	4.37
RC60 Bacteria	13530	1882	0.93	5.08
H10 Archaea	1405	68	0.99	2.76
H15 Archaea	5889	289	0.98	2.08
RC30 Archaea	2429	177	0.96	2.66
RC50 Archaea	2005	172	0.95	2.81
RC60 Archaea	2937	178	0.97	2.34

*Library coverage was calculated as C = 1-n/N, where n is the number of OTU_{97} without a replicate, and N is the total number of sequences.
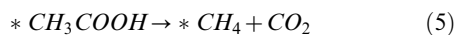**Shannon diversity index calculated using PAST.
doi:10.1371/journal.pone.0102456.t005

matter through acetate fermentation [47,110,112–115]. These processes can be described by the following reactions:

$$CO_2 + 8H^+ + 8e^- \rightarrow CH_4 + H_2O \qquad (4)$$

and

$$*CH_3COOH \rightarrow *CH_4 + CO_2 \qquad (5)$$

where the * indicates the intact transfer of the methyl position to CH4.

2) In the hypolimnion, microbial CH_4 production is still active, although this process is accompanied by CO_2 dissolution, CH_4 oxidation, and vertical diffusion of both the gas species. Moreover, in correspondence of aerobic/anaerobic boundaries, anaerobic decomposition of organic matter [116–118], and CH_4 oxidation carried out by methanotrophic bacteria can efficiently produce CO_2 in lakes [86,119–121].

3) In the epilimnion, photosynthetic microorganisms (e.g. *Cyanobacteria*) convert light into biochemical energy through oxygenic photochemical reactions combined with CO_2 assimilative reduction. Vertical water circulation favors the activity of photosynthetic and methanotrophic bacterial populations, as well as the continuous addition of atmospheric gases from the lake surface..

These hypotheses were confirmed by the 16S rRNA pyrosequencing of samples collected along the water column of Lake Rio Cuarto, demonstrating that archaeal communities encompass almost exclusively methanogenic populations (Tab. 7) typical of freshwater ecosystems, namely *Methanomicrobiales* and *Methanosarcinales* [122–124], as also observed in freshwater meromictic lake sediments [125]. *Methanosarcinales* included solely the acetate-utilizing methanogen *Methanosaeta*, the most abundant archaeal genus along the Río Cuarto water column. Within the H_2-CO_2 utilizing methanogens of the order *Methanomicrobiales*, *Methanoregula* was the prevalent genus, but unclassified *Methanomicrobiales* and *Methanoregulaceae* sequences were also detected (Tab. 7).

The lack of isotopic data along the vertical profile of Lake Hule did not allow to investigate in detail the (bio)-geochemical processes controlling the vertical profiles of CO_2 and CH_4. In this lake the majority of the archaeal 16S rRNA sequences were affiliated within unclassified Euryarchaeota, showing high similarity with the Candidate divisions Micrarchaea and Parvarchaea (Tab. 7) previously described by metagenomics studies of an acidic ecosystem by Baker *et al.* [126,127]. These archaeal sequences belong to the ARMAN (Archaeal Richmond Mine Acidophilic Nanoorganisms) lineages, which are among the smallest cellular life forms known [126], still poorly described from an ecological perspective. The presence of novel uncultivated lineages in the Lake Hule water is linked to neither specific metabolism nor the influence on the water and dissolved gas chemistry. However, besides a minor fraction of known acetotrophic methanogenic *Methanosarcinales* (Tab. 7), the archaeal community of Lake Hule included also the Miscellaneous Crenarchaeota Group (MCG), within the phylum Crenarchaeota (Tab. 7). MCG is a cosmopolitan clade that was previously detected in both freshwater [128] and marine ecosystems [129], where it had been hypothesized to have a significant role in dissimilatory methane oxidation [129]. This hypothesis leads to the speculation that MCG could have the same ecological function also in the Lake Hule. It is worth noting that the minor percentage of known methanogenic archaea in Lake Hule compared to that of Lake Río Cuarto corresponds to the differences between the lakes in CH_4 concentrations (Tab. 3).

16S rRNA pyrosequencing of bacterial communities showed that type I and type II methanotrophic bacteria, belonging to the Gamma- (i.e. *Methylocaldum*, *Methylomonas*, *Crenothrix*) and Alpha-subgroup of proteobacteria (i.e. *Methylocystaceae*) [125,130], respectively, were abundant in the anoxic layers of Hule and Río Cuarto (Tab. 6), suggesting a key role in the carbon cycle. Within the Beta-proteobacteria, additional families that encompass methylotrophic bacteria, namely *Methylophilaceae*, *Rhodocyclaceae*, and *Comamonadaceae* [131,132], were retrieved by deep sequencing in the same water layers both in Lake Hule and Lake Río Cuarto, the latter hosting up to 36% of *Methylophilaceae* at 30 m depth (Tab. 6). Within the family *Comamonadaceae*, relevant in Lake Hule, 5.2% of the bacterial sequences from the surface layer were affiliated to the genus *Limnohabitans*, which was reported to play a functional key role in freshwater habitats and showing high ecological diversification [133]. Moreover, 6.3% of the bacterial sequences were affiliated to the genus *Rubrivivax* that includes, among the few characterized

Table 6. List of the taxonomic groups, identified according to the results of the 16S rRNA pyrosequencing, composing the bacterial communities in the freshwater samples collected along the depth profiles of the Hule and Río Cuarto lakes.

PHYLUM/CLASS	ORDER	FAMILY	GENUS	H0	H10	H15	RC30	RC50	RC60
Other	Other	Other	Unknown seq	0.41	0.00	0.21	3.81	6.09	1.12
Other	Other	Other	Uncl. Bacteria	0.00	0.14	0.87	0.43	0.15	0.50
Acidobacteria	Uncl. Acidobacteria	Uncl. Acidobacteria	Uncl. Acidobacteria	0.00	0.13	1.15	0.00	0.00	0.00
Acidobacteria	Holophagales	Holophagaceae	Geothrix	0.00	2.79	3.87	0.00	0.00	0.00
Actinobacteria	Acidimicrobiales	Uncl. Acidimicrobiales	Uncl. Acidimicrobiales	0.25	0.08	0.33	3.55	0.78	0.71
Actinobacteria	Actinomycetales	ACK-M1	Uncl. ACK-M1	22.77	12.90	15.06	2.86	3.20	0.91
Actinobacteria	Actinomycetales	Microbacteriaceae	Candidatus Aquiluna	0.00	0.00	0.00	0.23	0.55	0.04
Actinobacteria	Uncl. Actinobacteria	Uncl. Actinobacteria	Uncl. Actinobacteria	0.00	0.00	0.01	0.21	0.01	1.15
Bacteroidetes	Uncl. Bacteroidetes	Uncl. Bacteroidetes	Uncl. Bacteroidetes	0.00	0.04	0.00	3.78	1.89	4.29
Bacteroidetes	Flavobacteriales	Cryomorphaceae	Uncl. Cryomorphaceae	3.32	0.00	0.00	0.00	0.00	0.00
Bacteroidetes	Flavobacteriales	Flavobacteriaceae	Flavobacterium	0.03	0.00	0.00	0.37	0.05	0.82
Bacteroidetes	Sphingobacteriales	Uncl. Sphingobacteriales	Uncl. Sphingobacteriales	0.00	0.00	0.00	2.19	11.55	0.22
Bacteroidetes	Sphingobacteriales	Chitinophagaceae	Uncl. Chitinophagaceae	2.29	0.42	0.24	0.00	0.00	0.00
Chlorobi	Chlorobiales	Chlorobiaceae	Uncl. Chlorobiaceae	0.00	14.40	10.96	0.12	0.08	0.11
Chlorobi	Ignavibacteriales	Other	Uncl. Ignavibacteriales	0.00	1.39	4.53	0.32	0.72	0.11
Chlorobi	Uncl. Chlorobi	Uncl. Chlorobi	Uncl. Chlorobi	0.00	2.77	2.11	6.71	3.57	5.83
Chloroflexi	Uncl. Anaerolineae	Uncl. Anaerolineae	Uncl. Anaerolineae	0.00	0.05	4.85	1.36	0.38	1.55
Chloroflexi	Uncl. Dehalococcoidetes	Uncl. Dehalococcoidetes	Uncl. Dehalococcoidetes	0.00	0.01	1.00	4.24	1.20	39.52
Cyanobacteria	Uncl. Cyanobacteria	Uncl. Cyanobacteria	Uncl. Cyanobacteria	0.01	0.00	0.01	1.01	2.89	0.07
Cyanobacteria	Synechococcales	Synechococcaceae	Prochlorococcus	29.4	2.56	1.45	17.19	40.20	1.47
OP3	Uncl. OP3	Uncl. OP3	Uncl. OP3	0.00	0.00	0.00	0.27	0.09	0.56
OP8	Uncl. OP8	Uncl. OP8	Uncl. OP8	0.00	0.00	0.00	0.05	0.00	1.20
Planctomycetes	Uncl. Phycisphaerae	Uncl. Phycisphaerae	Uncl. Phycisphaerae	0.00	0.00	0.00	0.36	0.15	0.14
Planctomycetes	Gemmatales	Gemmataceae	Uncl. Gemmataceae	0.16	0.06	0.67	0.65	0.76	0.87
Planctomycetes	Pirellulales	Pirellulaceae	Uncl. Pirellulaceae	0.57	0.39	0.72	2.06	1.03	3.39
Alphaproteobacteria	Rhizobiales	Methylocystaceae	Methylosinus	0.07	0.12	0.47	0.49	0.14	0.09
Alphaproteobacteria	Rhodospirillales	Rhodospirillaceae	Uncl. Rhodospirillaceae	0.04	0.97	1.14	0.08	0.04	0.01
Alphaproteobacteria	Rickettsiales	Uncl. Rickettsiales	Uncl. Rickettsiales	18.31	6.95	14.40	0.30	0.29	0.09
Betaproteobacteria	Uncl. Betaproteobacteria	Uncl. Betaproteobacteria	Uncl. Betaproteobacteria	0.00	0.00	0.00	0.58	0.23	0.36
Betaproteobacteria	Burkholderiales	Burkholderiaceae	Uncl. Burkholderiaceae	0.73	0.08	0.04	0.16	0.26	0.00
Betaproteobacteria	Burkholderiales	Comamonadaceae	Uncl. Comamonadaceae	3.22	0.29	0.44	0.02	0.02	0.00
Betaproteobacteria	Burkholderiales	Comamonadaceae	Limnohabitans	5.18	0.51	0.33	0.00	0.00	0.00
Betaproteobacteria	Burkholderiales	Comamonadaceae	Rhodoferax	4.59	0.12	0.24	0.00	0.00	0.00
Betaproteobacteria	Burkholderiales	Comamonadaceae	Rubrivivax	0.03	6.26	1.22	0.02	0.03	0.00

Table 6. Cont.

PHYLUM/CLASS	ORDER	FAMILY	GENUS	H0	H10	H15	RC30	RC50	RC60
Betaproteobacteria	Burkholderiales	Oxalobacteraceae	Uncl. Oxalobacteraceae	2.52	0.94	0.86	0.01	0.00	0.00
Betaproteobacteria	Burkholderiales	Oxalobacteraceae	Polynucleobacter	0.67	0.25	0.14	0.07	0.15	0.00
Betaproteobacteria	Methylophilales	Uncl. Methylophilales	Uncl. Methylophilales	0.70	1.01	0.32	0.00	0.00	0.00
Betaproteobacteria	Methylophilales	Methylophilaceae	Uncl. Methylophilaceae	0.03	4.21	2.72	35.99	11.75	20.57
Betaproteobacteria	Rhodocyclales	Rhodocyclaceae	Uncl. Rhodocyclaceae	0.00	1.05	0.36	0.91	2.13	0.09
Deltaproteobacteria	Desulfuromonadales	Geobacteraceae	Geobacter	0.00	0.00	0.01	0.24	0.04	0.66
Deltaproteobacteria	Myxococcales	Uncl. Myxococcales	Uncl. Myxococcales	0.00	0.00	0.98	0.07	0.03	0.06
Deltaproteobacteria	Spirobacillales	Uncl. Spirobacillales	Uncl. Spirobacillales	0.10	0.01	0.04	1.65	3.55	0.67
Deltaproteobacteria	Syntrophobacterales	Syntrophobacteraceae	Syntrophobacter	0.00	0.00	0.00	0.96	0.62	6.96
Epsilonproteobacteria	Campylobacterales	Helicobacteraceae	Sulfuricurvum	0.00	0.00	1.86	1.15	1.91	0.07
Gammaproteobacteria	Uncl. Gammaproteobacteria	Uncl. Gammaproteobacteria	Uncl. Gammaproteobacteria	0.00	0.00	0.00	0.44	1.72	0.10
Gammaproteobacteria	Enterobacteriales	Enterobacteriaceae	Uncl. Enterobacteriaceae	0.17	0.64	0.05	0.11	0.00	0.02
Gammaproteobacteria	Legionellales	Legionellaceae	Uncl. Legionellaceae	0.00	0.05	0.02	0.45	0.07	0.05
Gammaproteobacteria	Methylococcales	Crenotrichaceae	Crenothrix	0.00	17.25	3.37	0.00	0.00	0.00
Gammaproteobacteria	Methylococcales	Methylococcaceae	Methylocaldum	0.07	1.24	2.76	2.31	0.67	4.38
Gammaproteobacteria	Methylococcales	Methylococcaceae	Methylomonas	0.01	0.24	1.12	0.00	0.00	0.00
Gammaproteobacteria	Pseudomonadales	Pseudomonadaceae	Pseudomonas	0.01	16.31	16.47	0.00	0.02	0.02
Gammaproteobacteria	Xanthomonadales	Sinobacteraceae	Uncl. Sinobacteraceae	0.83	0.39	0.02	0.02	0.03	0.01
Verrucomicrobia	Opitutales	Opitutaceae	Opitutus	0.89	2.09	2.50	0.00	0.01	0.00
Verrucomicrobia	Uncl. Opitutae	Uncl. Opitutae	Uncl. Opitutae	2.61	0.89	0.06	0.00	0.04	0.00
Verrucomicrobia	Uncl. Verrucomicrobia	Uncl. Verrucomicrobia	Uncl. Verrucomicrobia	0.00	0.00	0.03	1.52	0.72	0.69
WS3	Uncl. WS3	Uncl. WS3	Uncl. WS3	0.00	0.00	0.00	0.64	0.22	0.47

Uncl: unclassified. Results are expressed as % of the sequences.
doi:10.1371/journal.pone.0102456.t006

Table 7. List of the taxonomic groups, identified according to the results if the 16S rRNA pyrosequencing, composing the archaeal communities in the freshwater samples collected along the depth profiles of the Hule and Río Cuarto lakes.

PHYLUM	CLASS	ORDER	FAMILY	GENUS	H10	H15	RC30	RC50	RC60
Unknown seq.	Unknown seq.	Unknown seq.	Unknown seq.	Unknown seq.	2.30	0.00	0.00	0.00	0.00
Uncl. Archaea	Uncl. Archaea	Uncl. Archaea	Uncl. Archaea	Uncl. Archaea	0.00	0.00	0.56	0.34	0.00
Crenarchaeota	MCG	Uncl. MCG	Uncl. MCG	Uncl. MCG	1.63	0.76	0.10	0.68	0.80
Crenarchaeota	MCG	pGrfC26	Uncl. pGrfC27	Uncl. pGrfC27	6.51	12.94	0.29	0.24	0.04
Euryarchaeota	Uncl. Euryarchaeota	Uncl. Euryarchaeota	Uncl. Euryarchaeota	Uncl. Euryarchaeota	0.95	0.30	0.00	0.00	0.00
Euryarchaeota	Methanomicrobia	Uncl. Methanomicrobia	Uncl. Methanomicrobia	Uncl. Methanomicrobia	0.00	0.00	0.10	0.43	0.18
Euryarchaeota	Methanomicrobia	Methanomicrobiales	Uncl. Methanoregulaceae	Uncl. Methanoregulaceae	0.50	0.32	0.62	1.21	0.55
Euryarchaeota	Methanomicrobia	Methanomicrobiales	Methanoregulaceae	Methanoregula	4.04	5.52	20.39	39.39	7.73
Euryarchaeota	Methanomicrobia	Methanosarcinales	Methanosaetaceae	Methanosaeta	1.01	0.92	46.67	39.59	86.48
Euryarchaeota	Cand. Micrarchaea	Cand. Micrarchaeles	Uncl. Micrarchaeles	Uncl. Micrarchaeles	25.01	73.09	29.84	14.32	3.72
Euryarchaeota	Cand. Parvarchaea	Cand. WCHD3-30	Uncl. WCHD3-30	Uncl. WCHD3-30	30.57	5.09	0.49	2.12	0.15
Euryarchaeota	Cand. Parvarchaea	Cand. YLA114	Uncl. YLA114	Uncl. YLA114	27.48	1.05	0.95	1.69	0.36

Uncl: unclassified. Cand: Candidatus. Results are expressed in % with respect to the total archaeal community.
doi:10.1371/journal.pone.0102456.t007

species, strains able to oxidize carbon monoxide producing carbon dioxide and hydrogen [134]. The presence of the genus *Syntrophobacter* at 60 m depth in Río Cuarto (RC60) is in agreement with the establishment in deep anoxic layers of syntrophic relations between organic acid degrading bacteria and methanogenic archaea. Members of this genus were commonly detected in anaerobic mixed cultures, where they obtain energy from the anaerobic oxidation of acetate, growing syntrophically with hydrogen- and formate-utilizing methanogenic archaea [135]. The RC60 sample showed a high percentage of sequences affiliated to the order Dehalococcoidetes (Tab. 6), which comprises obligate organohalide respirers, widely detected in marine and freshwater ecosystems [136,137]. The presence of organohalide compounds favors the competition with methanogens for the use of molecular hydrogen [138]. Hence the finding of Dehalococcoidetes in the deeper layers of Lake Río Cuarto, retrieved by both pyrosequencing (RC50) and DGGE (RC60), suggest the presence of naturally occurring organo-halogens in the water that could serve as electron acceptors for organohalide-respiring bacteria.

Further confirmation of the importance of anaerobic microbial processes on the CO_2-CH_4 balance can be obtained by comparing measured $\delta^{13}C_{TDIC}$ values with those expected assuming isotopic equilibrium between CO_2 and HCO_3^-. Isotopic fractionation caused by the reaction between dissolved CO_2 and HCO_3^- is quantified by the enrichment factor (ϵ_2), as follows [139]:

$$\epsilon_2 = \delta^{13}C - HCO_3^- - \delta^{13}C - CO_2 = 9483/T(K) - 23.9 \quad (6)$$

Theoretical $\delta^{13}C_{TDIC}$ values ($\delta^{13}C_{TDICcalc}$) can be computed by:

$$\delta^{13}C_{TDICcalc} =$$
$$\delta^{13}C - CO_2 + \epsilon_2 \times (HCO_3^-)/[(HCO_3^-) + (CO_2)] \quad (7)$$

As shown in Fig. 12, water samples from the shallower strata (down to 40 m depth) of Lake Río Cuarto displayed $\delta^{13}C_{TDIC}$ and $\delta^{13}C_{TDICcalc}$ values basically consistent. On the contrary, samples from depth >40 m showed a strong difference between the two sets of values: at −50 m depth, $\delta^{13}C_{TDICcalc}$ were more negative than $\delta^{13}C_{TDIC}$, whereas an opposite behavior was observed in the deeper water layer, as well as at the maximum depth of Lake Hule (Tab. 1). At the lake bottoms, continuous inputs of hydrothermal CO_2, characterized by $\delta^{13}C$-CO_2 values significantly less negative with respect to that already present in the lake, are likely responsible of the positive shift of the $\delta^{13}C_{TDICcalc}$ values, since this external CO_2 was not in equilibrium with HCO_3^-. In the shallower layers, especially at the depth of −60 m, addition of non-equilibrated biogenic CO_2 played an opposite role (Fig. 12), whereas at depth ≤40 m CO_2 concentrations were too low to significantly affect the $\delta^{13}C_{TDICcalc}$ values, which were consistent with the $\delta^{13}C_{TDIC}$ ones. The disagreement between measured and calculated $\delta^{13}C_{TDIC}$ values, depending on both microbial activity and inputs of hydrothermal CO_2, was documented in other meromictic lakes hosted in volcanic environments, such as Lake Kivu, D.R.C. [34] and the Italian lakes of Albano, Averno and Monticchio [86].

Although the multidisciplinary approach applied in the present study allowed to link the presence of different prokaryotic taxonomic groups to the observed physical conditions and the concentrations of chemical species along the water columns, the
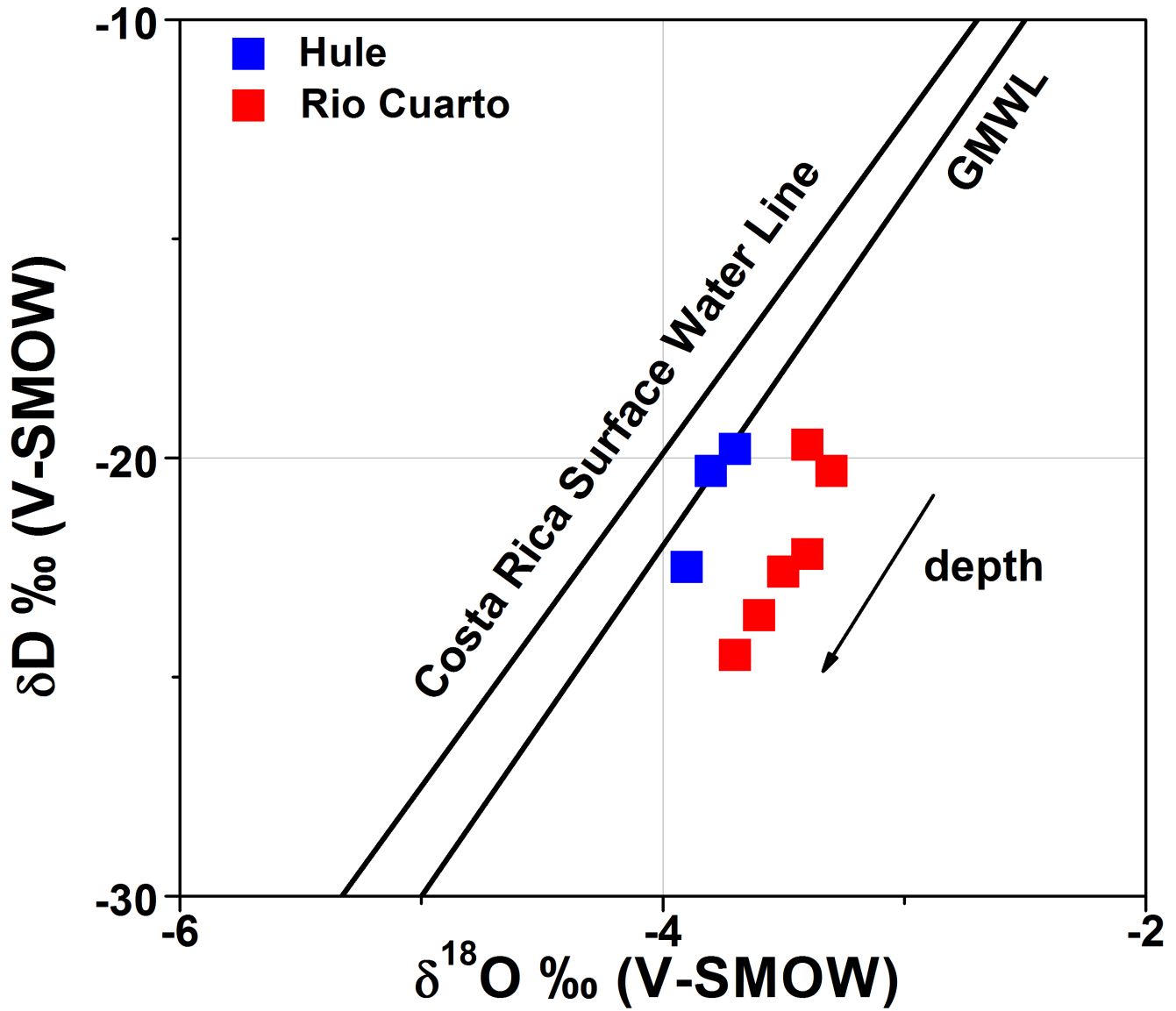
Figure 9. $\delta^{18}O$–δD diagram for the water samples from Lake Hule (blue squares) and Lake Río Cuarto (red squares). See the text for details.
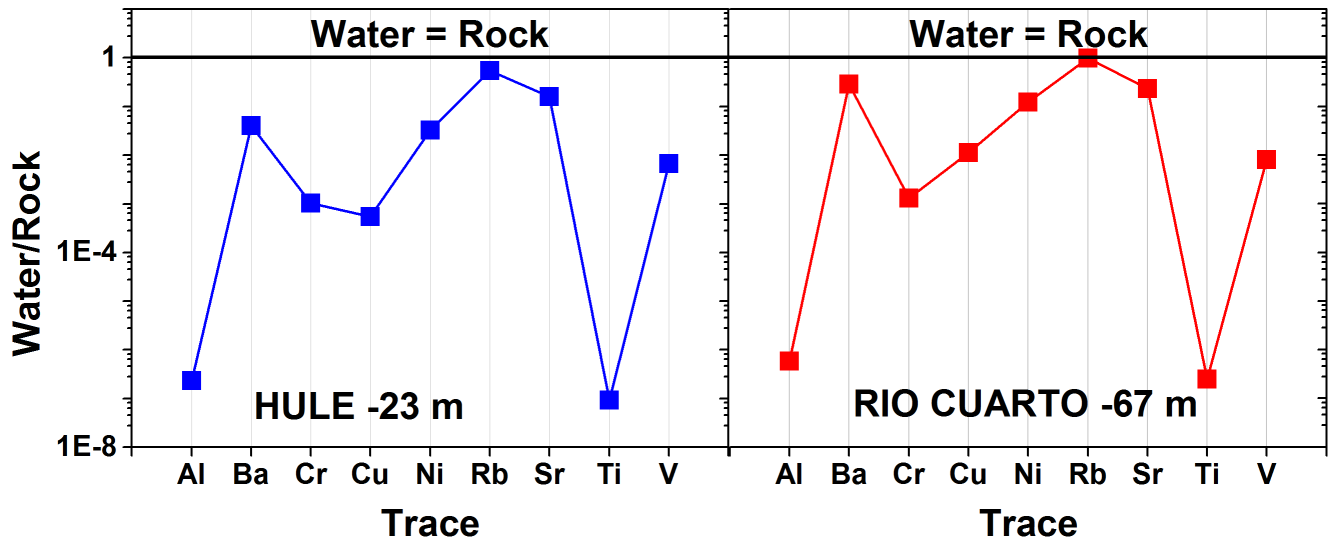doi:10.1371/journal.pone.0102456.g009

Figure 10. Spider-diagrams, where concentrations of selected trace elements in Lake Hule (a) and Lake Río Cuarto (b) maximum depths are normalized to those measured in basalt rock samples collected from the young intra-caldera cone at Laguna Hule [80].
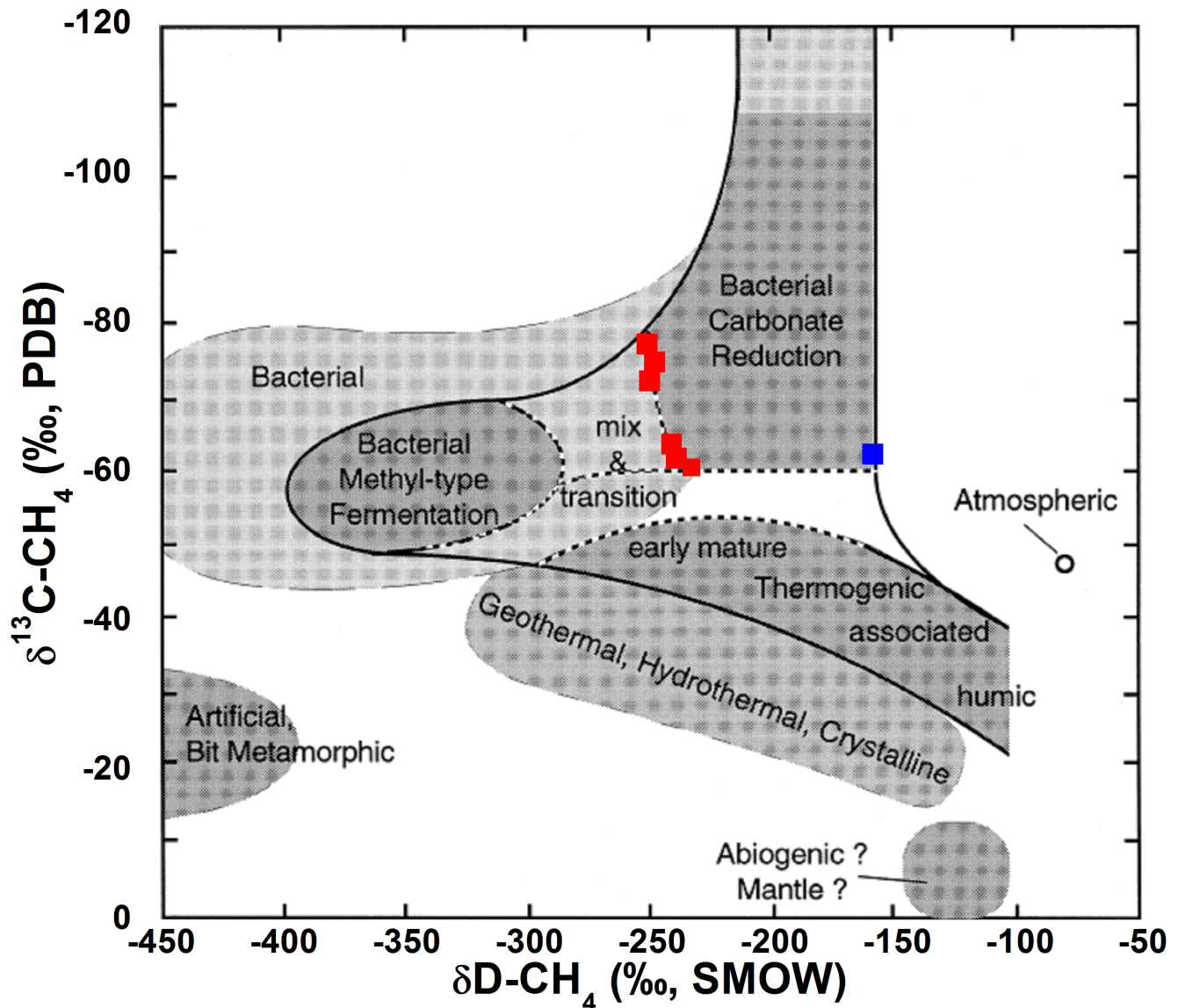doi:10.1371/journal.pone.0102456.g010

Figure 11. $\delta^{13}C\text{-}CH_4$ vs. $\delta D\text{-}CH_4$ plot (modified after Whiticar [110]) of Lake Hule (blue square) and Lake Río Cuarto (red squares). See the text for further details.
doi:10.1371/journal.pone.0102456.g011

ecological function of certain prokaryotes in these intriguing ecosystems, particularly in the case of Lake Hule, remains cryptic. In particular, among the bacterial community, Lake Hule hosted the Actinomycetales ACK-M1 cluster [140], whose phenotypic and metabolic traits have not yet been described. The ACK-M1 cluster was one of the most abundant bacterial taxonomic groups in Lake Hule, reaching up to 22.8% in the oxic water layer H0 (Tab. 6). Moreover, in the Lake Hule waters, the Alphaproteo-bacterial order Rickettsiales showed relatively high concentrations (18.3% of the total bacterial community in the oxic layer H0; Tab. 6). This order comprises intracellular organisms, pinpointing the importance of symbiotic relationships in these lakes. In this context, the impact of the associations between bacteria and algae [141] or phytoplancton [142] on nutrients re-mineralization was recently discussed showing the crucial role of trophic levels

interaction on the food web of lacustrine habitats, possibly relevant also in volcanic lakes.

Conclusions

Hule and Río Cuarto are meromictic maar lakes mainly fed by meteoric water, and characterized by significant amounts of dissolved gases, partially consisting of CO_2 having a hydrothermal-magmatic origin, in their hypolimnion. They are currently classified as low activity or, alternatively, "Nyos-type" lakes [4], implying that a limnic eruption could be expected to occur from these lakes, as confirmed by the rollover events they have experienced. However, gases stored in the deep layers of Hule and Río Cuarto are fundamentally different with respect to those of Nyos and Monoun lakes, a difference that must be considered for evaluating the eruption risk. The gas reservoirs of the two
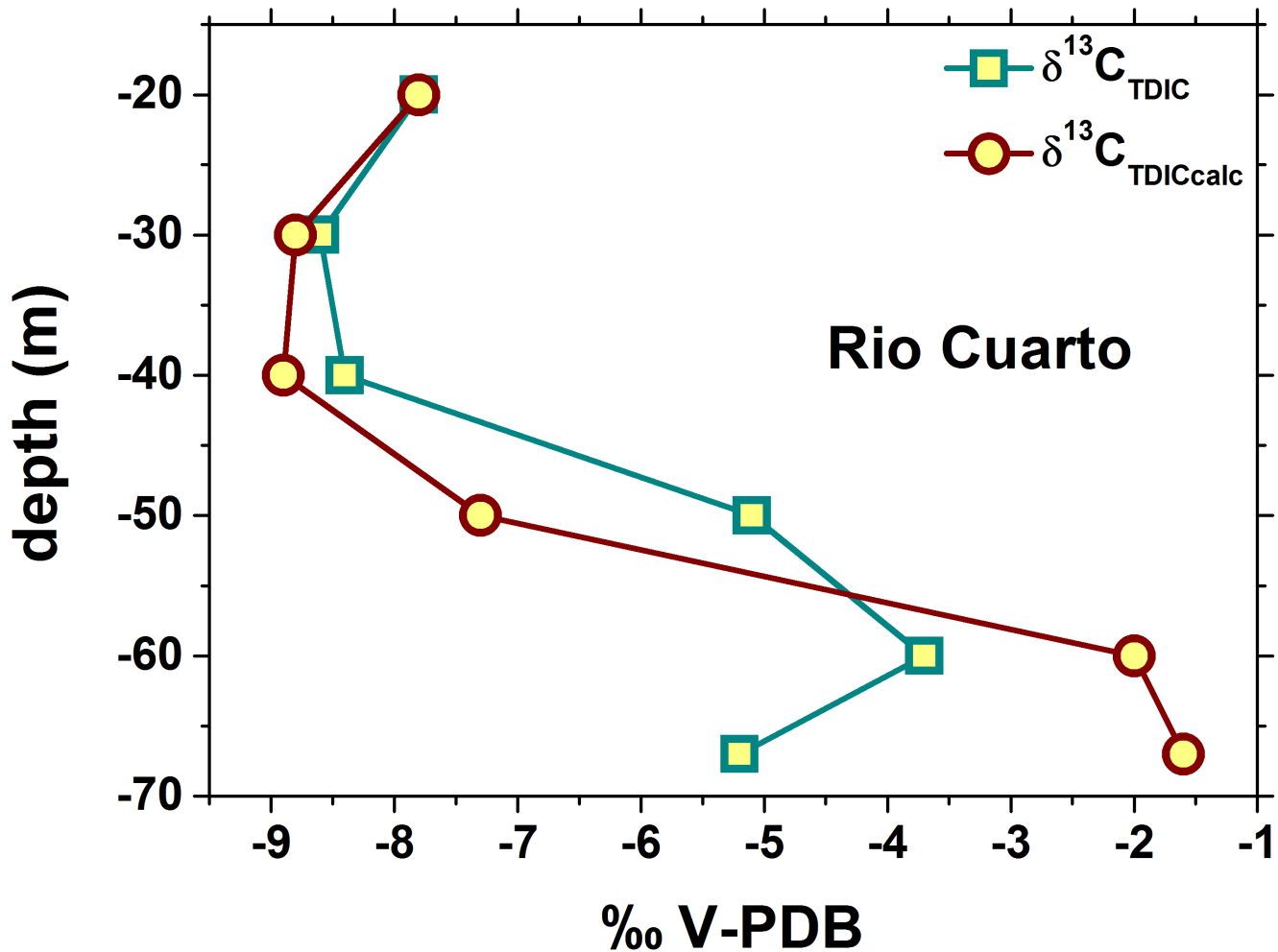
Figure 12. Vertical distribution of measured and calculated $\delta^{13}C_{TDIC}$ for the water samples from Lake Río Cuarto. See the text for further details.
doi:10.1371/journal.pone.0102456.g012

Cameroonian killer lakes are composed of almost pure CO_2 and basically their temporal evolution only depends on a high magmatic gas input rate [12,13]. At Nyos, the risk of gas bursts was successfully mitigated artificially by discharging the deep-seated gases at the lake surface [35,143]. On the contrary, the gas reservoirs of Hule and Río Cuarto lakes consist of CO_2, CH_4 and N_2 in comparable amounts, mainly controlled by the activity of a microbial network governed by CO_2 and CH_4 metabolism, thus the possible occurrence of a lake rollover that may pose a local risk is not directly related to the input rate of external CO_2.

Despite geographic separation, Lake Río Cuarto and Lake Hule showed similar physical-chemical settings, though hosting phylogenetically distinct bacterial and archaeal communities. Phylogenetic difference apart, however, both lakes have revealed the presence of the same prokaryotic ecological functions deeply involved in affecting water and gas chemistry.

On the whole, Lake Hule and Lake Rio Cuarto host a $CO_2(CH_4, N_2)$-rich gas reservoir which is mainly controlled by the complex and delicate interactions occurring between geosphere and biosphere and whose monitoring can appropriately be carried out by coupling the conventional geochemical approach with studies about prokaryotic colonization. Consequently, for these lakes we can introduce the new definition of *bio-activity* lakes. This term can be extended to several other volcanic lakes which show similar compositional features of water and dissolved gases, e.g. Kivu (D.R.C.-Rwanda) [34,144], Monticchio, Albano and Averno (Italy) [37,86,145–147], Pavin (France) [121,148].

Acknowledgments

Author Contributions

Conceived and designed the experiments: JC FT FM SB S. Calabrese DR GC RM BC RA OV GP S. Caliro RMA. Performed the experiments: JC FT FM SB S. Calabrese RM BC RA OV GP FC GB S. Caliro. Analyzed the data: JC FT FM SB. Contributed reagents/materials/analysis tools: FT SB S. Calabrese DR GC OV GP CR RMA. Contributed to the writing of the manuscript: JC FT FM SB S. Calabrese DR RM BC OV GP RMA.

23

References

1. Rouwet D, Tassi F, Mora-Amador R, Sandri L, Chiarini V (2014) Past, present and future of volcanic lake monitoring. J Volcanol Geotherm Res 272: 78–97.
2. Brown G, Rymer H, Dowden J, Kapadia P, Stevenson D, et al. (1989) Energy budget analysis for Poás crater lake: implications for predicting volcanic activity. Nature 339: 370–373.
3. Brantley SL, Agustsdottir AM, Rowe GL (1993) Crater lakes reveal volcanic heat and volatile fluxes. Geol Soc Am 3: 175–178.
4. Pasternack GB, Varekamp JC (1997) Volcanic lake systematics I. Physical constraints. Bull Volcanol 58(7): 528–538. doi:10.1007/s004450050160.
5. Anzidei M, Carapezza ML, Esposito A, Giordano G, Lelli M, et al. (2008) The Albano Maar Lake high resolution bathymetry and dissolved CO_2 budget (Colli Albani volcano, Italy): constrains to hazard evaluation. J Volcanol Geotherm Res 171: 258–268.
6. Hurst T, Christenson B, Cole-Baker J (2012) Use of a weather buoy to derive improved heat and mass balance parameters for Ruapehu Crater Lake. J Volcanol Geotherm Res 235: 23–28.
7. Rouwet D, Tassi F (2011) Geochemical monitoring of volcanic lakes. A generalized box model for active crater lakes. Ann Geophys 54: 161–173. doi:10.4401/ag-5035.
8. Kling GW, Clark MA, Compton HR, Devine JD, Evans WC, et al. (1987) The 1986 Lake Nyos gas disaster in Cameroon, West Africa. Science 236: 169–175.
9. Sigurdsson H, Devince JD, Tchoua FM, Presser TS, Pringle MKW, et al. (1987) Origin of the lethal gas burst from Lake Monoun, Cameroon. J Volcanol Geotherm Res 31: 1–16.
10. Barberi F, Chelini W, Marinelli G, Martini M (1989) The gas cloud of Lake Nyos (Cameroon, 1986): Results of the Italian technical mission. J Volcanol Geotherm Res 39: 125–134.
11. Giggenbach WF (1990) Water and gas chemistry of Lake Nyos and its bearing on the eruptive process. J Volcanol Geotherm Res 42: 337–362.
12. Evans WC, Kling GW, Tuttle ML, Tanyileke G, White LD (1993) Gas buildup in Lake Nyos, Cameroon: the recharge process and its consequences. Appl Geochem 8: 207–221.
13. Evans WC, White LD, Tuttle ML, Kling GW, Tanyileke G, et al. (1994) Six years of changes at Lake Nyos, Cameroon, yield clues to the past and cautions for the future. Geochem J 28: 139–162.
14. Kusakabe M (1996) Hazardous crater lakes. In: Scarpa R, Tilling RI, editors. Monitoring and mitigation of volcano hazards. Springer-Verlag, Berlin. pp. 573–598.
15. Rice A (2000) Rollover in volcanic crater lakes: a possible cause for Lake Nyos type disasters. J Volcanol Geotherm Res 97: 233–239.
16. Haberyan KA, Horn SP, Umaña GV (2003) Basic limnology of fifty-one lakes in Costa Rica. Rev Biol Trop 51: 107–122.
17. Tassi F, Vaselli O, Fernandez E, Duarte E, Martinez M, et al. (2009b) Morphological and geochemical features of crater lakes in Costa Rica: an overview. J Limnol 68: 193–205.
18. Alvarado GE, Soto GJ, Salani FM, Ruiz P, Hurtado de Mendoza L (2011) The formation and evolution of Hule and Río Cuarto maars, Costa Rica. J Volcanol Geotherm Res 201: 342–356.
19. Horn SP, Haberyan KA (1993) Physical and chemical properties of Costa Rican lakes. Natl Geogr Res Explor 9(1): 86–103.
20. Horn SP (2001) The age of the Laguna Hule explosion crater, Costa Rica, and the timing of subsequent tephra eruptions: evidence from lake sediments. Rev Geol Am Cent 24: 57–66.
21. Umaña G, Haberyan KA, Horn SP (1999) Limnology in Costa Rica. In: Gopal B, Wetzel RW, editors. Limnology in Developing Countries 2: 33–62.
22. Haberyan KA, Horn SP (1999) Chemical and physical characteristics of seven volcanic lakes in Costa Rica. Brenesia 51: 85–95.
23. Umaña G (1993) The planktonic community of Laguna Hule, Costa Rica. Rev Biol Trop 41(3): 499–507.
24. Göcke K (1997) Basic morphometric and limnological properities of Laguna Hule, a caldera lake in Costa Rica. Rev Biol Trop 44/45: 537–548.
25. Göcke K, Bussing W, Cortés J (1987) Morphometric and basic limnological properties of the Laguna de Río Cuarto, Costa Rica. Rev Biol Trop 35(2): 277–285.
26. Carpenter SR (1983) Lake geometry: implications for production and sediment accretion rates. J Theor Biol 105: 273–286.
27. Lehman JT (1975) Reconstructing the rate of accumulation of lake sediment. The effect of sediment focusing. Quatern Res 5: 541–550.
28. Martini M, Giannini L, Prati F, Tassi F, Capaccioni B, et al. (1994) Chemical characters of crater lakes in the Azores and Italy: the anomaly of the Lake Albano. Geochem J 28: 173–184.
29. Wetzel RG (2001) Limnology: Lake and River Ecosystems. 3rd Ed., Academic, San Diego, Calif., USA.
30. Soto GJ (1999) Geología Regional de la hoja Poás (1: 50.000). In: Alvarado GE, Madrigal LA, editors. Estudio Geológico-Geotécnico de Avance a factibilidad del P. Laguna Hule. Inf. Interno ICE, San José, Costa Rica. pp. 15–45.
31. Sapper K (1925) Los Volcanes de la América Central. Max Niemayer, Halle (Saale). 144 p.
32. Göcke K, Bussing W, Cortés J (1990) The annual cycle of primary productivity in Laguna de Río Cuarto, a volcanic lake (maar) in Costa Rica. Rev Biol Trop 38(2B): 387–394.
33. Tassi F, Vaselli O, Giannini L, Tedesco D, Nencetti A, et al. (2004) A low-cost and effective method to collect water and gas samples from stratified crater lakes: the 485 m deep lake Kivu (DRC). Proc. IAVCEI Gen. Ass., Puchon, Chile, 14–19 November 2004.
34. Tassi F, Vaselli O, Tedesco D, Montegrossi G, Darrah T, et al. (2009a) Water and gas chemistry at Lake Kivu (DRC): geochemical evidence of vertical and horizontal heterogeneities in a multi-basin structure Geochem. Geophys. Geosyst. 10, doi:10.1029/2008GC002191
35. Tassi F, Rouwet D (2014) An overview of the structure, hazards, and methods of investigation of Nyos-type lakes from the geochemical perspective. J Limnol 73(1): DOI: 10.4081/jlimnol.2014.836
36. Chiodini G (1996) Gases dissolved in groundwaters: analytical methods and examples of applications in central Italy. In: Marini L, Ottonello G, editors. Proc. Symp. Environmental Geochemistry. Castelnuovo di Porto, Rome, 22–26 May 1996. pp. 135–148.
37. Caliro S, Chiodini G, Izzo G, Minopoli C, Signorini A, et al. (2008) Geochemical and biochemical evidence of lake overturn and fish kill at Lake Averno, Italy. J Volcanol Geotherm Res 178: 305–316.
38. Tassi F, Vaselli O, Luchetti G, Montegrossi G, Minissale A (2008) Metodo per la determinazione dei gas disciolti in acque naturali. Int Rep CNR-IGG, Florence, n° 10450. 11 p.
39. Calabrese S, Aiuppa A, Allard P, Bagnato E, Bellomo S, et al. (2011) Atmospheric sources and sinks of volcanogenic elements in a basaltic volcano (Etna, Italy). Geochim Cosmochim Acta 75: 7401–7425.
40. Epstein S, Mayeda TK (1953) Variation of the $^{18}O/^{16}O$ ratio in natural waters. Geochim Cosmochim Acta 4: 213–224.
41. Nelson ST (2000) A simple, practical methodology for routine VSMOW/SLAP normalization of water samples analyzed by continuous flow methods. Rapid Commun Mass Spectrom 14: 1044–1046.
42. Salata GG, Roelke LA, Cifuentes LA (2000) A rapid and precise method for measuring stable carbon isotope ratios of dissolved inorganic carbon. Mar Chem 69: 153–161.
43. Evans WC, White LD, Rapp JB (1998) Geochemistry of some gases in hydrothermal fluids from the southern Juan de Fuca ridge. J Geophys Res 15: 305–313.
44. Vaselli O, Tassi F, Montegrossi G, Capaccioni B, Giannini L (2006) Sampling and analysis of fumarolic gases. Acta Vulcanol 1–2: 65–76.
45. Whitfield M (1978) Activity coefficients in natural waters. In: Pytkowicz RM, editor. Activity Coefficients in Electrolyte Solutions. CRC Press, Boca Raton, Florida, pp. 153–300.
46. Zhang J, Quay PD, Wilbur DO (1995) Carbon isotope fractionation during gas-water exchange and dissolution of CO_2. Geochim Cosmochim Acta 59: 107–114.
47. Schoell M (1980) The hydrogen and carbon isotopic composition of methane from natural gases of various origins. Geochim Cosmochim Acta 44: 649–661.
48. Mamyrin BA, Tolstikhin IN (1984) Helium isotopes in nature. Elsevier, Amsterdam.
49. Ozima M, Podosek FA (2002) Noble Gas Geochemistry. Cambridge University Press, UK.
50. Inguaggiato S, Rizzo A (2004) Dissolved helium isotope ratios in ground-waters: a new technique based on gas-water re-equilibration and its application to Stromboli volcanic system. Appl Geochem 19: 665–673. http://dx.doi.org/10.1016/j.apgeochem.2003.10.009
51. Mapelli F, Varela MM, Barbato M, Alvariño R, Fusi M, et al. (2013) Biogeography of planktonic microbial communities across the whole Mediterranean Sea. Ocean Sci Discuss 10: 291–319. doi:10.5194/osd-10-291-2013
52. Marasco R, Rolli E, Ettoumi B, Vigani G, Mapelli F, et al. (2012) A drought resistance-promoting microbiome is selected by root system under desert farming. PLoS ONE 7(10): e48479. doi:10.1371/journal.pone.0048479
53. Harhangi HR, Le Roy M, van Alen T, Hu B-I, Groen J, et al. (2012) Hydrazine synthase, a unique phylomarker with which to study the presence and biodiversity of anammox bacteria. Appl Environ Microbiol 78: 752–758.
54. Van de Peer Y, Chapelle S, De Wachter R (1996) A quantitative map of nucleotide substitution rates in bacterial rRNA. Nucleic Acids Res 24(17): 3381–3391.
55. Chakravorty S, Helb D, Burday M, Connell N, Alland D (2007) A detailed analysis of 16S ribosomal RNA gene segments for the diagnosis of pathogenic bacteria. J Microbiol Methods 69: 330–339.
56. Caporaso JG, Kuczynski J, Stombaugh J, Bittinger K, Bushman FD, et al. (2010) QIIME allows analysis of high-throughput community sequencing data. Nat Methods 7: 335–336.
57. Edgar RC (2010) Search and clustering orders of magnitude faster than BLAST. Bioinformatics 26(19): 2460–2461.
58. Wang Q, Garrity GM, Tiedje JM, Cole JR (2007) Naïve Bayesian Classifier for Rapid Assignment of rRNA Sequences into the New Bacterial Taxonomy. Appl Environ Microbiol 73(16): 5261–5267.
59. Hammer Ø, Harper DAT, Ryan PD (2001) PAST: paleontological statistics software package for education and data analysis. Palaeontol Electronica 4(4): 1–9.

60. Umaña G (2010) Comparison of basic limnological aspects of some crater lakes in the Cordillera Volcánica Central, Costa Rica. Rev Geol Amér Central 43: 137–145.

61. Craig H, Lupton JE (1976) Primordial neon, helium and hydrogen in oceanic basalts. Earth Planet Sci Lett 31: 369–385.

62. Wu QL, Zwart G, Schauer M, Kamst-van Agterveld MP, Hahn MW (2006) Bacterioplankton Community Composition along a Salinity Gradient of Sixteen High-Mountain Lakes Located on the Tibetan Plateau, China. AEM 72: 5478–5485.

63. Zhu G, Jetten MSM, Kuschk P, Ettwig KF, Yin C (2010) Potential roles of anaerobic ammonium and methane oxidation in the nitrogen cycle of wetland ecosystems. Appl Microbiol Biotechnol 86: 1043–1055.

64. Varekamp JC, Kreulen R (2000) The stable isotope geochemistry of volcanic lakes, with examples from Indonesia. J Volcanol Geotherm Res 97: 309–327.

65. Craig H (1961) Isotopic variations in meteoric waters. Science 133: 1702–1703.

66. Lachniet MS, Patterson WP (2002) Stable isotope values of Costa Rican surface waters. J Hydrol 260: 135–150.

67. Berner EK, Berner RA (1987) Global Water Cycle: Geochemistry and Environment. Prentice-Hall, Inc, Englewood Cliffs, New Jersey. p. 397.

68. Matsubaya O, Sakai H (1978) D/H and $^{18}O/^{16}O$ fractionation factors in evaporation of water at 60 and 80°C. Geochem J 12: 121–126.

69. Rowe GL Jr (1994) Oxygen, hydrogen and sulfur isotope systematics of the crater lake system of Poas volcano, Costa Rica. Geochem J 28: 263–287.

70. Alexander M (1961) Introduction to Soil Microbiology. John Wiley & Sons, New York. p. 472.

71. Buresh RJ, Patrick WH (1981) Nitrate reduction to ammonium and organic nitrogen in an estuarine sediment. Soil Biol Biochem 13: 279–283.

72. Stewart WDP, Preston T, Peterson HG, Christofi N (1982) Nitrogen cycling in eutrophic freshwaters. Philosoph Transact Royal Soc B 296: 491–509.

73. Ahlgren I, Sörensson F, Waara T, Vrede K (1994) Nitrogen budgets in relation to microbial transformations in lakes. Ambio 23(6): 367–377.

74. Brune A, Frenzel P, Cypionka H (2000) Life at the oxic-anoxic interface: microbial activities and adaptation. FEMS Microbiol Rev 24(5): 691–710.

75. Carlson CA, Ingraham JL (1983) Comparison of denitrification by *Pseudomonas stutzeri*, *Pseudomonas aeruginosa*, and *Paracoccus denitrificans*. Appl Environ Microbiol 45: 1247–1253.

76. Molongoski JJ, Klug MJ (1980) Anaerobic metabolism of particulate organic matter in the sediments of a hypereutrophic lake. Freshwater Biol 10: 507–518.

77. Davison W, Heaney SI, Talling JF, Rigg E (1980) Seasonal transformations and movements of iron in a productive English lake with deep water anoxia. Schweiz Z Hydrol 42: 196–224.

78. Balistrieri LS, Murray JW, Paul B (1992) The cycling of iron and manganese in the water column of Lake Sammamish, Washington. Limnol Oceanogr 37: 510–528.

79. Hongve D (1997) Cycling of iron, manganese, and phosphate in a meromictic lake. Limnol Oceanogr 42: 635–647.

80. Prosser JT, Carr MJ (1987) Poás volcano, Costa Rica: geology of the summit region and spatial and temporal variations among the most recent lavas. J Volcanol Geotherm Res 33: 131–146.

81. Balistrieri LS, Murray JW, Paul B (1994) The geochemical cycling of trace elements in a biogenic meromictic lake. Geochim Cosmochim Acta 58(19): 3993–4008.

82. Viollier E, Jezequel D, Michard G, Pepe M, Sarazin G, et al. (1995) Geochemical study of a crater lake (Pavin Lake, France): trace-element behaviour in the monimolimnion. Chem Geol 125(1–2): 61–72.

83. Schaller T, Moor HC, Wehrli B (1997) Reconstructing the iron cycle from the horizontal distribution of metals in the sediment of Baldeggersee. Aquat Sci 59: 326–344.

84. Varekamp JC, Pasternack GB, Rowe GL Jr (2000) Volcanic lake systematics II. Chemical constraints. J Volcanol Geotherm Res 97: 161–179.

85. Schmid M, Halbwachs M, Wehrli B, Wüest A (2005) Weak mixing in Lake Kivu: new insights indicate increasing risk of uncontrolled gas eruption. Geochem Geophys Geosyst 6: 1–11.

86. Cabassi J, Tassi F, Vaselli O, Fiebig J, Nocentini M, et al. (2013) Biogeochemical processes involving dissolved CO_2 and CH_4 at Albano, Averno, and Monticchio meromictic volcanic lakes (Central-Southern Italy). Bull Volcanol 75(1): 1–19.

87. Weiss R (1970) The solubility of nitrogen, oxygen and argon in water and seawater. Deep Sea Res 17: 721–735.

88. Tison DL, Palmer FE, Staley JT (1977) Nitrogen fixation in lakes of the Lake Washington drainage basin. Water Res 11: 843–847.

89. Hyenstrand P, Blomqvist P, Pettersson A (1998) Factors determining cyanobacterial success in aquatic systems – a literature review. Arch Hydrobiol 15: 41–62.

90. Moeller RE, Roskoski JP (1978) Nitrogen-fixation in the littoral benthos of an oligotrophic lake. Hydrobiologia 60(1): 13–16.

91. Loeb SL, Reuter JE (1981) The epilithic periphyton community: a five-lake comparative study of community productivity, nitrogen metabolism and depth-distribution of standing crop. Verh Internat Verein Limnol 21: 346–352.

92. Valiela I (1991) Ecology of coastal ecosystems. In: Barnes RSK, Mann KH, editors.Fundamentals of aquatic ecology. Blackwell Science, Oxford, pp. 57–76.

93. Benemann JR, Weare NM (1974) Hydrogen evolution by nitrogen-fixing *Anabaena cylindrical* cultures. Science 184: 174–175.

94. Greenbaum E (1982) Photosynthetic hydrogen and oxygen production: kinetic studies. Science 215: 291–293.

95. Asada Y, Kawamura S (1986) Aerobic hydrogen accumulation by a nitrogen-fixing Cyanobacterium, *Anabaena* sp. Appl Environ Microbiol 51: 1063–1066.

96. Asada Y, Miyake J (1999) Photobiological hydrogen production. J Biosci Bioengineer 88(1): 1–6.

97. Bandyopadhyay B, Stöckel J, Min H, Sherman LA, Pakrasi HB (2010) High rates of photobiological H_2 production by a cyanobacterium under aerobic conditions. Nature Communications 1: 139. doi:10.1038/ncomms1139

98. Mah RA, Ward DM, Baresi L, Glass TL (1977) Biogenesis of methane. Annu Rev Microbiol 31: 309–341.

99. Zehnder AJB (1978) Ecology of methane formation. In: Michell R, editor. Water pollution microbiologyk. J. Wiley & Sons Inc, New York. pp. 349–376.

100. Thauer RK, Badziong W (1980) Respiration with sulfate as electron acceptor. In: Knowles CJ, editor.Diversity of bacterial respiratory systems. CRC Press, Boca Raton, Fla, 2. pp. 65–85.

101. Aragno M, Schlegel HG (1981) The hydrogen-oxidizing bacteria. In: Starr MP, Stolp H, Trüper HG, Ballows A, Schlegel HG, editors.The prokaryotes. A handbook of habitats, isolation and identification of bacteria. Vol. 1. Springer-Verlag, Berlin.

102. Bowien B, Schlegel HG (1981) Physiology and biochemistry of aerobic hydrogen-oxidizing bacteria. Ann Rev Microbiol 35: 405–452.

103. Conrad R, Aragno M, Seiler W (1983) Production and consumption of hydrogen in a eutrophic lake. Appl Environ Microbiol 45: 502–510.

104. Bianchi L, Mannelli F, Viti C, Adessi A, De Philippis R (2010) Hydrogen-producing purple non-sulfur bacteria isolated from the trophic lake Averno. Int J Hydr En 35: 12213–12223.

105. Zimmer MM, Fisher TP, Hilton DH, Alvarado GE, Sharp ZD, et al. (2004) Nitrogen systematics and gas fluxes of subduction zones: insights from Costa Rica arc volatiles. Geochem Geophys Geosyst 5(5): 1–19. doi:10.1029/2003GC000651

106. Barnes I, Irwin WP, White DE (1978) Global distribution of carbon dioxide discharges and major zones of seismicity. US Geological Survey, Water-Resources Investigation, 78–39, Open File Report.

107. O'Leary MH (1988) Carbon isotopes in photosynthesis. BioScience 38: 328–336.

108. Rollinson H (1993) Using geochemical data: evaluation, presentation, interpretation. Longman Scientific and Technical, New York, p. 352.

109. Hoefs J (2009) Stable Isotope Geochemistry, 6th edn. Springer, Berlin, Germany, p. 288.

110. Whiticar MJ (1999) Carbon and hydrogen isotope systematics of bacterial formation and oxidation of methane. Chem Geol 161: 291–314.

111. Alvarado GE, Soto GJ, Pullinger CR, Escobar R, Bonis S, et al. (2007) Volcanic activity, hazards, and monitoring. In: Bundschuh J, Alvarado GE, editors.Central America: Geology, Resources and Hazards, Vol. 2. Taylor & Francis, London, pp. 1155–1188.

112. Mah RA, Ward DM, Baresi L, Glass TL (1977) Biogenesis of methane. Annu Rev Microbiol 31: 309–341.

113. Barker JF, Fritz P (1981) Carbon isotope fractionation during microbial methane oxidation. Nature 293: 289–291.

114. Schoell M (1988) Multiple origins of methane in the Earth. Chem Geol 71: 1–10.

115. Woese CR, Kandler O, Wheelis ML (1990) Towards a natural system of organisms: proposal for the domains Archaea, Bacteria and Eucarya. Proc Natl Acad Sci 87: 44576–44579.

116. Rudd JWM, Hamilton RD, Campbell NER (1974) Measurement of microbial oxidation of methane in lake water. Limnol Oceanogr 19: 519–524.

117. Rich PH (1975) Benthic metabolism of a soft-water lake. Verh Internat Verein Limnol 19: 1023–1028.

118. Rich PH (1980) Hypolimnetic metabolism in three Cape Cod lakes. Amer Midland Natur 104: 102–109.

119. Frenzel P, Thebrath B, Conrad R (1990) Oxidation of methane in the oxic surface layer of a deep lake sediment (Lake Constance). FEMS Microbiol Ecol 73: 149–158.

120. Casper P (1992) Methane production in lakes of different trophic state. Arch Hydrobiol Beih Ergebn Limnol 37: 149–154.

121. Lopes F, Viollier E, Thiam A, Michard G, Abril G, et al. (2011) Biogeochemical modeling of anaerobic vs. aerobic methane oxidation in a meromictic crater lake (Lake Pavin, France). Appl Geochem 26: 1919–1932.

122. Franzmann PD, Liu YT, Balkwill DL, Aldrich HC, deMacario EC, et al. (1997) *Methanogenium frigidum* sp. nov., a psychrophilic, H_2-using methanogen from Ace Lake, Antarctica. Int J Syst Bacteriol 47: 1068–1072.

123. Bräuer SL, Cadillo-Quiroz H, Ward RJ, Yavitt JB, Zinder SH (2011) Methanoregula boonei gen. nov., sp. nov., an acidiphilic methanogen isolated from an acidic peat bog. Int J Syst Evol Microbiol 61: 45–52.

124. Chaudhary PP, Brablcová L, Buriánková I, Rulík M (2013) Molecular diversity and tools for deciphering the methanogen community structure and diversity in freshwater sediments. Appl Microbiol Biotechnol 97: 7553–7562.

125. Borrel G, Jézéquel D, Biderre-Petit C, Morel-Desrosiers N, Morel J, et al. (2011) Production and consumption of methane in freshwater lake ecosystems. Res Microbiol 162: 832–847.

126. Baker BJ, Tyson GW, Webb RI, Flanagan J, Hugenholtz P, et al. (2006) Lineages of acidophilic Archaea revealed by community genomic analysis. Science 314: 1933–1935. doi:10.1126/science.1132690.

127. Baker BJ, Comolli LR, Dicka GJ, Hauser LJ, Hyatt D, et al. (2010) Enigmatic, ultrasmall, uncultivated Archaea. PNAS 107: 8806–8811.

128. Borrel G, Lehours A-C, Crouzet O, Jézéquel D, Rockne K, et al. (2012) Stratification of Archaea in the deep sediments of a freshwater meromictic lake: Vertical Shift from Methanogenic to Uncultured Archaeal Lineages. PLoS ONE 7:e43346. doi:10.1371/journal.pone.0043346.

129. Biddle JF, Lipp JS, Lever MA, Lloyd KG, Sørensen KB, et al. (2006) Heterotrophic Archaea dominate sedimentary subsurface ecosystems off Peru. PNAS 103: 3846–3851.

130. Stoecker K, Bendinger B, Schöning B, Nielsen PH, Nielsen JL, et al. (2006) Cohn's Crenothrix is a filamentous methane oxidizer with an unusual methane monooxygenase. PNAS 103: 2363–2367.

131. Chistoserdova L, Kalyuzhnaya MG, Lidstrom ME (2009) The expanding world of methylotrophic metabolism. Annu Rev Microbiol 63: 477–499. doi:10.1146/annurev.micro.091208.073600

132. Beck DAC, Kalyuzhnaya MG, Malfatti S, Tringe SG, del Rio TG, et al. (2013) A metagenomic insight into freshwater methane-utilizing communities and evidence for cooperation between the *Methylococcaceae* and the *Methylophilaceae*. PeerJ 1:e23. doi:10.7717/peerj.23

133. Jezbera J, Jezberová J, Kasalický V, Šimek K, Hahn MW (2013) Patterns of *Limnohabitans* microdiversity across a large set of freshwater habitats as revealed by reverse line blot hybridization. PLoS ONE 8: e58527. doi:10.1371/journal.pone.0058527.

134. Maness P, Huang J, Smolinski S, Tek V, Vanzin G (2005) Energy generation from the CO oxidation-hydrogen production pathway in *Rubrivivax gelatinosus*. Appl Environ Microbiol 71: 2870–2874.

135. Harmsen HJM, Van Kuijk BLM, Plugge CM, Akkermans ADL, De Vos WM, et al. (1998) *Syntrophobacter furnaroxidans* sp nov, a syntrophic propionate-degrading sulfate-reducing bacterium. Int J Syst Bact 48: 1383–1387.

136. Hug LA, Castelle CJ, Wrighton KC, Thomas BC, Sharon I, et al. (2013) Community genomic analyses constrain the distribution of metabolic traits across the Chloroflexi phylum and indicate roles in sediment carbon cycling. Microbiome 1:22, doi:10.1186/2049-2618-1-22.

137. Zanaroli G, Balloi A, Negroni A, Borruso L, Daffonchio D, et al. (2012) A Chloroflexi bacterium dechlorinates polychlorinated biphenyls in marine sediments under in situ-like biogeochemical conditions. J Haz Mat 209–210: 449–457.

138. Balloi A, Rolli E, Marasco R, Mapelli F, Tamagnini I, et al. (2010) The role of microorganisms in bioremediation and phytoremediation of polluted and stressed soils. Agrochimica 54(6): 353–369.

139. Mook WG, Bommerson JC, Staverman WH (1974) Carbon isotope fractionation between dissolved bicarbonate and gaseous carbon dioxide. Earth Planet Sci Lett 22: 169–176.

140. Zwart G, Crump BC, Agterveld M, Hagen F, Han SK (2002) Typical freshwater bacteria: an analysis of available 16S rRNA gene sequences from plankton of lakes and rivers. Aquat Microb Ecol 28: 141–155.

141. Eigemann F, Hilt S, Salka I, Grossart H (2013) Bacterial community composition associated with freshwater algae: species specificity vs. dependency on environmental conditions and source community. FEMS Microbiol Ecol 83: 650–663.

142. Paver SF, Hayek KR, Gano KA, Fagen JR, Brown CT, et al. (2013) Interactions between specific phytoplankton and bacteria affect lake bacterial community succession. Environ Microbiol 15: 2489–2504.

143. Kusakabe M, Ohba T, Issa YY, Satake H, Ohizumi T, et al. (2008) Evolution of CO_2 in lakes Monoun and Nyos, Cameroon, before and during controlled degassing. Geochem J 42: 93–118.

144. Schoell M, Tietze K, Schoberth SM (1988) Origin of methane in Lake Kivu (East-Central Africa). Chem Geol 71: 257–265.

145. Carapezza ML, Lelli M, Tarchini L (2008) Geochemistry of the Albano and Nemi crater lakes in the volcanic district of Alban Hills (Rome, Italy). J Volcanol Geotherm Res 178: 297–304.

146. Caracausi A, Nuccio PM, Favara R, Nicolosi M, Paternoster M (2009) Gas hazard assessment at the Monticchio crater lakes of Mt Vulture, a volcano in Southern Italy. Terra Nova 21: 83–87.

147. Chiodini G, Tassi F, Caliro S, Chiarabba C, Vaselli O, et al. (2012) Time-dependent CO_2 variations in Lake Albano associated with seismic activity. Bull Volcanol 74: 861–871.

148. Aeschbach-Hertig W, Hofer M, Kipfer R, Imboden DM, Wieler R (1999) Accumulation of mantle gases in a permanently stratified volcanic lake (Lac Pavin, France). Geochim Cosmochim Acta 63: 3357–3372.